Pop-up archival tags reveal environmental influences on the vertical movements of silvertip sharks (*Carcharhinus albimarginatus*).

David M Tickler[1]*, Aaron B Carlisle[2], Jessica J Meeuwig[1], Taylor K Chapple[3,4], David Curnick[5], Jonathan J Dale[4], Michael J Castleton[4], Robert J Schallert[4], Barbara B Block[4]

1. Oceans Institute: Centre for Marine Futures, University of Western Australia, 35 Stirling Highway, Crawley, Perth, WA 6009, Australia
2. School of Marine Science and Policy, University of Delaware, Lewes, DE, 19958, USA
3. Coastal Oregon Marine Experiment Station, Oregon State University, Newport, OR, 97365, USA
4. Hopkins Marine Station of Stanford University, Pacific Grove, CA 93950, United States of America
5. Institute of Zoology, Zoological Society of London, Regent's Park, London, NW1 4RY, U.K.

* Corresponding author

Abstract

Vertical space use informs the ecology and management of marine species, but studies of reef-associated sharks often focus on horizontal movements. We analysed the vertical movements of silvertip sharks (*Carcharhinus albimarginatus*) using pop-up archival tags deployed on seven individuals in the Chagos Archipelago, central Indian Ocean. The sharks changed depth predictably with water column thermal structure, moving deeper with seasonal increases mixed layer depth while occupying a narrow ambient water temperature range around ~27°C. At shorter timescales, higher resolution data from five tags showed that silvertip shark depth varied cyclically with surface light levels, increasing during daylight and on nights around full moon. This matches the diel vertical migration of many fish species, suggesting the sharks' light-driven depth changes might relate to foraging. While most vertical movements (>98%) were within the mixed layer, deeper dives to 200-800 m occurred approximately every three days. High-resolution dive data from one recovered tag showed the shark ascending from its maximum depth in two sharply defined phases, fast then slow. Analysis of dive profiles against dissolved oxygen (DO) data suggested that the shark may have ascended rapidly to escape low DO levels at depth, then reduced its ascent rate 50-80% once DO levels increased. While a small sample, the pop-up tags deployed in this study revealed the silvertip sharks' predictable use of mixed layer waters, narrow thermal range and

apparent intolerance of hypoxic conditions. These characteristics may exacerbate the species' vulnerability as oceanic warming and shoaling oxygen minimum zones modify vertical habitat availability.

Keywords: Coral reef, Mini-PAT, Oxygen threshold, Silvertip shark, Spatial ecology, Telemetry, Thermal tolerance, Diving behaviour

1. Introduction

Sharks are an important group of marine predators, but both pelagic and reef-associated species are under threat (Baum & Myers 2004, Graham et al. 2010, Ferretti et al. 2010, Worm & Tittensor 2011, Nadon et al. 2012, MacNeil et al. 2020). Population declines of many species have been observed globally, with fisheries (Meekan et al. 2006, Vianna et al. 2016) and habitat degradation (Knip & Heupel 2010, Sguotti et al. 2016) identified as key drivers. Sharks are also likely to be impacted by the effects of climate change, including ocean warming and reductions in dissolved oxygen availability (Chin et al. 2010, Gilly et al. 2013, Rosa et al. 2017).

Knowledge of sharks' spatial ecology improves our understanding of their ecosystem roles (Williams et al. 2018) and vulnerability to threats (Jacoby et al. 2020), and aids in designing conservation strategies (Chapman et al. 2005, Lea et al. 2016, Dwyer et al. 2020). While data on the horizontal movements of sharks provides important insights, a full understanding of the ecology of many species requires information on their vertical space use (Andrzejaczek et al. 2019, 2022). Sharks' vertical movements may be an important dimension of their role in connecting ecosystems and food webs, for example by mediating nutrient transfers between surface, meso- and bathypelagic layers (Roman & McCarthy 2010, Braun et al. 2014, Howey et al. 2016). Vertical space use also influences species' exposure to human threats, including their likelihood of interacting with different fishing gears (Vedor 2021a).

Species' vertical space use may be driven by, *inter alia*, water temperature and thermoregulation needs (Sims et al. 2006, Campana et al. 2011), dissolved oxygen (DO) levels (Carlson 2003, Carlisle et al. 2016), and diel cycles in prey distribution and behaviour (Bost et al. 2002, Baumgartner et al. 2011). Modelling species' vertical space use with respect to environmental factors, such as temperature, oxygen availability and light-levels, can therefore provide insights into their ecology and biology, revealing cryptic behaviours such as foraging or aggregating at depth (Cagua et al. 2015, Braun et al. 2019), and physiological constraints such as temperature and DO thresholds (Abascal et al. 2011, Carlisle et al. 2015).

Highly mobile shark species are commonly studied with pop-up satellite archival tags (hereafter PATs), which collect data on ambient pressure (i.e., depth), temperature and light levels (used to infer horizontal movements). Summary data are normally transmitted (via

satellite) after the tag detaches from the animal, but a full data archive can be also downloaded from any physically recovered tags (Hammerschlag et al. 2011, Block et al. 2011, Hussey et al. 2015). Satellite tagging studies have been conducted on many mobile shark species, including oceanic white tip (*Carcharhinus longimanius*, Andrzejaczek et al. 2018, Tolotti et al. 2017), blue (*Prionace glauca*, Campana et al. 2011), white (*Carcharodon carcharias*, Jorgensen et al. 2012), salmon (*Lamna ditropis*, Carlisle et al. 2011), porbeagle (*Lamna nasus*, Francis et al. 2015), basking (*Cetorhinus maximus*, Doherty et al. 2019), six-gill (*Hexanchus griseus*, Coffey et al. 2020), tiger (*Galeocerdo cuvier*, Heithaus et al. 2007, Afonso and Hazon 2015), silky (*Carcharhinus falciformis,* Curnick et al. 2020b), whale (*Rhincodon typus*, Araujo et al. 2019), mako (*Isurus* spp.), and thresher sharks (*Alopias* spp., Block et al. 2011). These studies have provided many insights into the vertical lives of the species studied, such as residency to the relatively warm surface mixed layer (Tolotti et al. 2017), ontogenetic differences in depth use (Afonso and Hazin 2015) and the characteristics of diving behaviour (Howey et al. 2016). Nominally resident species, such as reef-associated sharks, are more commonly studied with passive acoustic telemetry, with movements inferred from detections of acoustically tagged animals within an array of acoustic receivers. While acoustic tagging can also provide depth and temperature data (e.g., Vianna et al. 2013, Espinoza et al. 2015a), its collection relies on animals being within detection range, and continuous high-resolution data can be difficult to acquire. Much of the research on reef-associated sharks to date has therefore focussed on quantifying aspects of horizontal space use such as habitat associations, movement networks and home ranges (e.g. Donaldson et al. 2014, Espinoza et al. 2015b, White et al. 2017, Jacoby et al. 2020).

To date, few studies have used PAT tags to study the vertical space use of reef-associated sharks (Andrzejaczek et al. 2022). This may be driven by the high cost of the individual tags, relative to their perceived utility for species thought to exhibit relatively restricted movements and diving behaviours. Compared to pelagic taxa, PAT tags have so far been deployed sparingly on reef-associated species: on a single silvertip shark (*Carcharhinus albimarginatus*) in Fiji (Bond et al. 2015), 16 grey reef sharks (*Carcharhinus amblyrhynchos*) in the Marshall Islands (Bradley et al. 2019), and six Caribbean reef sharks (*Carcharhinus perezi*) in Belize (Chapman et al. 2007). However, the high-resolution depth and temperature time series generated by the PATs has allowed these studies to generate insights beyond the

capabilities of acoustic telemetry. These include describing a much larger vertical and thermal niche than previously suspected for Caribbean reef sharks (Chapman et al. 2007), and providing direct evidence of offshore mesopelagic diving in silvertip sharks (Bond et al. 2015).

In the current study we used PATs to investigate the vertical space use of silvertip sharks in the central Indian Ocean. Silvertip sharks are a large, mobile reef-associated species, with a wide but fragmented distribution throughout the Indo-Pacific (Compagno 1984). They are listed as Vulnerable by the IUCN (Espinoza et al. 2016) and populations appear to have been seriously impacted by fishing in several parts of its range (Meekan et al. 2006, Graham et al. 2010, Ferretti et al. 2018). Silvertip sharks are reported to dive up to 800 m (Compagno 1984), and a short deployment of a PAT tag on a silvertip shark in Fiji found that the animal occupied a depth range of 0-380 m, with a mean depth of ~60 m and an average water temperature of 26.3 °C, cooler than the shallows (Bond et al. 2015). Similarly, a 2012 survey around the Chagos Archipelago in the BIOT, using baited remote underwater video, found that while silvertip sharks were present across a broad depth range (15 to 80 m) they were at higher abundance, relative to grey reef sharks, on deeper sites (Tickler et al. 2017). This apparent deeper depth distribution may have biased earlier attempts to model silvertip shark abundance and population trends based on shallow visual surveys or fishing (e.g. Ferretti et al. 2018), and better knowledge of their spatial ecology might better inform abundance surveys and models used to infer their conservation status. Additionally, the silvertip shark has been relatively under-studied compared with its smaller congener, the grey reef shark, and improved knowledge of its spatial ecology could help to better inform its conservation management.

Here we analyse data from PATs deployed in 2013 and 2014 on seven silvertip sharks within the large marine protected area (MPA) that surrounds the Chagos Archipelago in the British Indian Ocean Territory (BIOT). The overall goal of this study was to describe the vertical space use of silvertip sharks in relation to physical drivers including sea surface temperature, water column structure, and solar and lunar illumination, to better predict temporal variations in its susceptibility to fishing gears (e.g. surface longlines), and to identify any thermal or other constraints that might provide insight into this species' vulnerability to ocean warming under climate change. We examined temporal variation in the depth use of sharks in relation to sea surface temperature and the depth of the surface mixed layer, since both have been shown

to drive vertical space use in other mobile ectothermic shark species (Campana et al. 2011, Howey et al. 2016). We also investigated the influence of diel and lunar cycles which have both been shown to predict depth use in multiple species including the grey reef shark (Vianna et al. 2013), silky shark (Curnick et al. 2020b), blue shark (Queiroz et al. 2010) and blacktip reef shark (*C. melanopterus*, Papastamatiou et al. 2018). Lastly, we investigated the relationship between diving behaviour and water column stratification (temperature, DO), which are known to influence the diving behaviour of other species that make mesopelagic excursions (such as the oceanic whitetip shark; Howey et al. 2016).

2. Methods

2.1. Study area

The Chagos Archipelago comprises a group of atolls, islands and seamounts in the central Indian Ocean, centred on ~6.5° S, ~72° E (Figure 1). Due to its geographical isolation and protected status within the BIOT MPA, the reefs and surrounding waters are considered a valuable location at which to investigate the ecology of both reef and pelagic sharks under conditions of very low anthropogenic disturbance (Hays et al. 2020). The area's climate is defined by two monsoon seasons: the summer (northwest) monsoon from December to March, characterised by light west-northwesterly winds, warmer temperatures and more rainfall, and the winter (southwest) monsoon from June to September, with stronger south-easterly winds and cooler drier weather. Periods in between the monsoons tend to have calm weather with light and variable winds. The majority of the BIOT EEZ which surrounds the Archipelago, an area totalling over 640,000 km^2, is a no-take MPA, although a 3 nm zone around the military base at the southern atoll of Diego Garcia is excluded. The area has been largely unpopulated since the 1970s, with the exception of the military base, and since the MPA's creation in 2010 all commercial fishing and other extractive activities have been prohibited, with only very limited subsistence fishing for finfish by visiting yachts remains permitted within the MPA.

2.2. Pop-up archival tags

Seven PAT tags (MiniPAT-247 model tags, Wildlife Computers, Redmond WA) were used in this study. Since data recovery from PATs via the Argos satellite network is constrained by tag battery life and satellite coverage, a range of configurations of data resolution and deployment time was used to increase the likelihood of obtaining useable data (Table 1). The PATs recorded ambient temperature, depth and light level at 15 s intervals and were programmed to detach after 120, 180 or 270 days (Table 1). Tags were programmed to transmit their temperature and depth data summarized as time-at-depth (TAD) and time-at-temperature (TAT) histograms, in 6- or 24-hour intervals. The histogram data were reported as the proportion of time spent in each of 12 pre-defined depth or temperature bins during each 6- or 24-hour period (Supplementary Tables S1 and S2). A subset of tags were

programmed to transmit time series of their depth and temperature data sampled at 5-minute or 7.5-minute intervals (Table 1). Tags also reported summarised light level data, for geolocation purposes, daily temperature-at-depth profiles (PDT), minimum and maximum depth in each reporting period, and daily estimates of Mixed Layer Depth (MLD). The PDT data contain the minimum and maximum temperature recorded at 8 or 16 depth increments, set dynamically between the minimum and maximum depth recorded on a given day. Prior to deployment, each tag was prepared with anti-fouling paint (Trilux 33; International Paint LLC, Union, NJ, USA), and attached to a custom-made titanium dart using 15 cm of 180 kg monofilament leader (Moimoi, Kobe, Japan). The leader material was protected from abrasion with a layer of Spectra (Honeywell Advanced Fibres and Composites, Colonial Heights, VA, USA) and covered with a length of heatshrink tubing.

2.3. Tag deployment

Seven silvertip sharks were tagged around the Chagos Archipelago in the BIOT MPA in February/March 2013 (four tags) and March 2014 (three tags). Tags were deployed on sharks caught around the Peros Banhos and Salomon atolls and near the submerged features at Benares Shoals, Blenheim Reef and Victory Bank (Figure 1b). Sharks were captured using barbless 16/0 circle hooks, attached to a wire leader (1 m of 3 mm steel wire rope) joined to 2 m of 10-15 mm polypropylene line with a swivel, and terminated with a large longline branch hanger ('tuna clip'). These hook sets were baited with pieces of squid and deployed either singly, clipped to a weighted polypropylene drop line, or in sets of up to 10 at a time clipped at 15 m intervals to a floating polypropylene surface line. Once a shark was hooked, it was brought alongside the tagging vessel and a soft tail rope was secured just anterior to the caudal fin. Animals larger than approximately 1.5 m were left in the water and turned ventral side up to induce tonic immobility (Kessel & Hussey 2015). Smaller individuals were lifted onto a large vinyl padded mat and restrained. While sharks were out of the water, their gills were irrigated via a perforated plastic pipe attached to a seawater pump, and their eyes were covered with a wet cloth to further reduce stress. The PATs were attached externally by inserting the dart into the dorsal musculature just below the dorsal fin. The dart was inserted at a shallow angle relative to the axis of the shark's body, from the tail towards the head, to minimise drag from the tag. In all cases precaudal (PCL), fork (FL) and total (TL) lengths were measured to the nearest cm, a fin clip from a pectoral fin was taken for DNA analysis, and a

muscle punch taken for stable isotope analysis. One shark (Tag 6, ID 391401600) was tagged with both a PAT and an acoustic tag (V16 model tag, Vemco, Halifax, Nova Scotia). The acoustic tag was inserted into the abdominal cavity of the shark via a small incision, made posterior to the pectoral fins and just off the ventral midline (Haulsee et al. 2016), and closed with a single non-absorbable nylon suture (3-0, 24 mm) using a reverse cutting needle (Ethicon, US). Animals were also tagged externally with a conventional "spaghetti" type identification tag, so that tagged animals could be identified if recaptured. The conventional tag was inserted in to the dorsal musculature on the opposite side to the PAT anchor to avoid entanglement between the tags. All sharks were tagged and released within five minutes.

2.4. Tag recovery and data pre-processing

Six of the seven PATs were not recovered after releasing from their sharks, but transmitted subsets of their data via the Argos satellite network. The remaining tag (Tag 1, ID 391300800; Table 1) was physically recovered after drifting to the Kenyan coast, post-release, and provided a 180-day dataset of depth and temperature measurements at 15 second intervals. Raw data transmitted by the PATs via the Argos satellites were processed using Wildlife Computers' Data Analysis Program (DAP; Wildlife Computers, Redmond, WA, USA). This resulted in daily summaries of TAD, TAT, PDT, SST, minimum/maximum depth (MinMaxDepth) and light levels. Data times in UTC were converted to the local time zone (UTC+5). Four tags generated data summaries at 24-hour intervals, of which two also transmitted portions of their time series data, sampled at 5-minute and 7.5-minute intervals (Table 1), and the remaining two tags generated data summaries at six-hour intervals, at 0000, 0600, 1200 and 1800 UTC.

Five of the seven tags also reported MLD estimates based on the depth and temperature data (Table 1). For the two tags that did not provide MLD estimates, we used the method of Kara et al. (2000) to generate estimates of the isothermal layer depth (approximating the MLD) directly from the tag data, by analysing temperature changes with depth. Briefly, the Kara algorithm searches the depth-temperature profile from the surface downwards until it finds a point where the change in temperature with depth exceeds a defined threshold, in this case 1.5°C (Kara et al. 2000). The isothermal layer depth is defined as the depth at which the difference between the ambient temperature and the inferred mixed layer temperature first

exceeds this threshold (Kara et al. 2000). The 1.5°C temperature change threshold was chosen after calibrating the Kara algorithm against MLD estimates from the tags.

Daily geolocation position estimates for the tags were generated based on light level data and SST using the method of Teo et al. (2004). The algorithm uses changing ambient light levels to identify local times of dawn and dusk and calculate day length, related to latitude, and time of local noon, related to longitude (Hill & Braun 2001). Light-based geolocation position estimates were then validated by comparing *in situ* SST measurements from the tag with remote-sensed SST distributions (Teo et al. 2004). The resulting position estimates were refined using a state-space model which takes into account additional data on local cloud cover and bathymetry (Block et al. 2011, Winship et al. 2011). Daily estimated positions and associated errors (95% confidence intervals) were generated for each tag track.

Data from the V16 acoustic tag were collected using an array of Vemco acoustic receivers (VR2 type, Vemco, Halifax, Nova Scotia) deployed around the reefs in the northern part of the Chagos Archipelago in 2013 and 2014 (Supplementary Figure S1). The methods used to deploy, anchor and retrieve the acoustic receivers have been described in detail in earlier studies (e.g. Tickler et al. 2019, Carlisle et al. 2019, Williamson et al. 2021)

2.5. Data analysis

All statistical analysis was performed using R Statistical Software (version 3.5.1; R Core Team). Homogeneity of variance for parametric tests (t-test and ANOVA) was tested using Levene's Test. The results of statistical tests were considered statistically significant at the 5% level if the p-value of the associated test statistic was < 0.05.

2.5.1. Shark horizontal movements

Shark tracks, and associated error ellipses based on the 95% confidence intervals of estimated longitude and latitude, were overlaid on a map of the BIOT MPA to visualise shark movements with respect to their tagging locations, the atolls of the Chagos Archipelago, and the BIOT MPA boundary. Data from a single shark tagged with both a PAT and a passive acoustic tag was also used to investigate variation in geolocation errors over time. Methods and results for this exploratory analysis are included in the Supplementary Material.

2.5.2. Individual tag depth versus water column temperature profiles

To compare data across all seven tags, we aggregated all TAD and TAT histogram data to 24-hour periods, averaging across shorter 6-hour summaries where necessary. For each tag, we calculated the median, interquartile range (IQR) and 95% range for depth and temperature for each daily summary by linearly interpolating within the depth and temperature bin ranges to estimate the depth or temperature value for each quantile. Where upper bin boundaries for depth and temperature were open (i.e., > 500 m or > 32°C, respectively; Supplementary Tables 1 and 2) they were assumed to be 1000 m and 34°C, respectively.

We reconstructed water column thermal profiles, or bathythermographs, over time from each tag's daily depth and temperature profiles, i.e. PDT records. We created the bathythermograph data from each tag's PDT records by first averaging the minimum and maximum temperatures for each depth step reported in the PDT, and then interpolating temperature linearly between the depth steps to infer the temperature at two metre intervals. This produced a depth/temperature raster with two metre vertical resolution for each tag and date; i.e. if a tag reported mean temperatures of 28°C at 10 m and 26°C at 18 m, the temperature was assumed to be 27.75°C at 12 m, 27.50°C at 14 m, etc. In this way each two-metre increment in the daily depth-temperature profile was assigned a temperature intermediate between the reported values for the large depth steps. For the single tag for which high-resolution (15 s) pairs of depth and temperature records were available (Tag 1, ID 391300800), bathythermograph data were obtained by averaging the temperature records within two-metre depth bins, i.e. 0-2 m, 2-4 m, etc. for each 24-hour period.

We plotted each shark's bathythermograph and superimposed the median depth +/- IQR to visualise the relationship between each shark's depth and the water column thermal structure over time. We calculated the Pearson correlation between the median daily depth of the sharks and the daily estimates of mixed layer depth to quantify the strength of the relationship.

2.5.3. Median depth and temperature by month for all sharks

The reported summary histograms of (proportion of) time-at-depth and-time-at temperature used different bin boundaries to summarise the data from different tags (Supplementary Tables S1 and S2). To calculate summary statistics for all tag data pooled together, we

289 therefore first recalculated the histogram data for all tags based on a single set of depth and
290 temperature bins. This allowed us to directly compare, and average, the proportion of time
291 spent in each depth or temperature bin across tags. All data histograms were re-calculated
292 using the depth and temperature histogram bin boundaries for Tag 1, with maximum depth
293 and temperature values set to 1000 m and 34°C, respectively (Supplementary Tables S1 and
294 S2). The proportion of time spent in given depth and temperature bins was re-allocated to
295 the new bins on the assumption that time spent between two given depths or temperatures
296 was uniformly distributed. Having standardised the histogram data, we pooled the data
297 across tags by day and calendar month and calculated overall median depth and temperature
298 for each day. We then compared trends in the sharks' median daily depth and ambient
299 temperature, by calendar month, with median MLD and SST, respectively, using box plots. As
300 the variance of the observations varied significantly between months, variation in mean
301 depth by calendar month was tested using Welch's ANOVA, using the oneway.test() function,
302 with pairwise comparisons between months made using Tukey's test in the
303 games_howell_test() function.

304 *2.5.4. Diel and lunar variations in depth and temperature*

305 For the five tags with data recorded either as 6-hour histograms or as time series (Table 1),
306 we aggregated depth and temperature data by date and diel period (TOD), classified as *day* if
307 data were recorded between approximately 6am to 6pm local time, otherwise *night*. Lunar
308 phase (new, waxing, full, waning) was assigned to each record based on date, using the
309 function lunar.phase() in the R package *lunar* (Lazaridis 2014). For the data stored as
310 histograms, summary depth and temperature statistics (median, IQR and 95% range) were
311 calculated for each period for each date using the same interpolation methodology as
312 described above for the 24 hr histograms. Quantile values for the time series data were
313 calculated using the R base function *quantile()*. We also calculated the mean percentage of
314 time, ± 95% confidence interval, that sharks spent below depth thresholds (75, 100, 150 m)
315 and temperature thresholds (25, 22, 18°C), overall and by diel period. Day vs. night
316 differences in the mean proportions of time spent below these temperature and depth
317 thresholds were tested using t-tests.

318 To test for an effect of time of day and lunar phase on shark median depth, independent of
319 seasonal changes in overall depth, we first calculated the difference between the median

depth in each period (day or night) and a rolling 30-day median depth for each tag. Analysis of variance was then used to test for significant effects of time of day and lunar phase, and the interaction between them, on seasonally-adjusted median depth. We used Tukey's test to test for significant differences between levels of interaction between time of day and lunar phase.

2.5.5. Mixed modelling of median depth against environmental factors

We modelled the median daily depth of each shark against environmental factors for the five tags with TOD data using generalised linear mixed-effects modelling (GLMM, Bolker et al. 2009) with Gaussian error structure and identity link function, implemented in the function lme() in the R package *nlme* (Pinheiro et al. 2018). The dataset included 962 date/TOD depth records for 481 days of data. Fixed predictors were Mixed layer depth (MLD, in metres), sea surface temperature (SST, in °C), lunar phase (moon: new, waxing, full, waning) and TOD , with tag ID (identifying individual sharks) included as a random effect. We also tested the interaction between TOD and moon to test the hypothesis that depth changes were related to light levels in the water column, i.e. to test for an effect of moonlight levels at night. The significance of the random intercept (1|TagID) was tested using the methodology of Zuur et al. (2009). The AICc and log-likelihood scores of a model without random effects were compared to those of a mixed model in which the random effect term was included. The significance of the additional random effect term was evaluated based on the likelihood ratio test in the function anova(). Collinearity between the fixed predictors was checked by calculating Generalised Variance Inflation Factors (GVIF) using the vif.lme() function from the package *spida15* (Monette 2012). The GVIF values were all ≤1.01, indicating low collinearity between predictors (Supplementary Table S3).

Model building was performed using forward selection following the method of Kock et al. (2013), starting from a null model with random effect only and adding and combining predictors sequentially. The explanatory power of each model was evaluated using the Akaike information criterion, corrected for sample size, (AICc), and a likelihood ratio test (LRT) was used to compare the best models at each level of complexity (single-variable, two-variable, etc.). This approach was favoured over more complex machine-learning approaches, e.g. Boosted Regression Trees (Elith et al. 2008), in order to both find the most parsimonious model and maintain ease of interpretation. Model residuals were tested for over-dispersion

using the testDispersion() function in the *DHARMa* package (Hartig 2022) and temporal autocorrelation was checked using the ACF() function in base R, using the option 'resType = "normalized"'. There was no evidence of over-dispersion (Supplementary Figure S2) but a plot of residuals against time and the ACF plot both showed evidence of temporal autocorrelation (Supplementary Figures S3, S4). We added a second order autoregressive term using CorARMA() with the parameter 'p' set to two, and rechecked the ACF plot to confirm that the autocorrelation had been correctly accounted for (Supplementary Figure S4). Model selection process was then re-run with the CorARMA() term included with models ranked by AICc as before. A summary table of all model variants tested was generated using the model.sel() function in the package *MuMIn* (Multi-model Inference, Bartoń 2022). For models within four points of the lowest AICc (i.e. ΔAICc < 4) we used the r.squaredGLMM() function in *MuMIn* to calculate marginal R^2 and conditional R^2 so that the variance explained by fixed and fixed-plus-random predictors could be compared (Schielzeth and Nakagawa 2013). Diagnostic plots (residuals vs fitted values, scale-location, residuals against time and Q-Q plots) were used to visualise the fit of the final model selected and check that assumptions of normality were not violated.

2.5.6. Investigation of individual diving behaviour (Tag 1, ID 391300800)

The depth-time series from the recovered PAT (Tag 1, ID 391300800) contained 180 days of continuous 15-second interval depth records, allowing individual dives to be identified in the time series. The threshold for dives below the mixed layer was assumed to be 100 m since this was the maximum MLD found in the data, and the sharks spent > 98% of their time above this depth. Detailed analyses focussed on mesopelagic dives below 200 m, since depth-time plots of these deeper dives showed two distinct phases in the ascent portion of the dives, marked by a sharp reduction in ascent rate (hereafter transition point, sensu Howey 2016; Figure S5a), which warranted further investigation.

We defined a custom window function (Supplementary Material Part C) to identify the time and depth of discontinuities in the ascent trajectory of each dive (hereafter transition points). A transition point was defined as an instantaneous reduction in ascent rate of at least 50%, before and after which the ascent rate had been relatively constant for at least one minute. The window function was initialised at the start of each dive's ascent (i.e. after the deepest

point) and then moved through the remaining depth-time series in increments of 15 s (i.e. one time-step in the tag data). The date, time and depth of qualifying points in the dive profiles were recorded. To visualise the transition point dives, we standardised the time axis of each dive profile by defining the transition point of each depth-time series as t = 0, and calculated the mean depth at each (relative) time step across all dive profiles.

Temperature data for each dive were obtained directly from the tag data. Climatological dissolved oxygen (DO) values for the study area were downloaded from the NOAA World Ocean Atlas (WOA, https://www.nodc.noaa.gov/cgi-bin/OC5/woa13/woa13oxnu.pl, monthly means, 1 degree latitude/longitude resolution). The WOA data provide average vertical DO profiles at 5m to 50 m resolution. The dataset's vertical resolution decreases with depth: 25m resolution from 100 m to 500 m, 50 m resolution from 500 m to 1500 m. To generate DO profiles for each dive, we first interpolated vertically within each WOA record to get DO values at 10 m intervals. We then interpolated horizontally and temporally between locations and dates in the WOA DO data to estimate values for the locations and dates of the shark's individual dives. An approximate location for each dive was assumed from the tag's geolocation estimate for the corresponding day. Given the low spatial resolution of the WOA data, the accuracy of the geolocation estimates was not thought to be a significant additional source of error in estimating DO values for the dives. Spatial interpolation between dive locations and the grid centroids in the WOA dataset was performed with the R package *akima*, using a cubic-spline interpolation based on the method of Akima et al. (1978). We assumed that the monthly averages in the WOA data corresponded to the 15th day of each month, and we then used a linear interpolation to estimate DO values on the date of each dive.

We investigated potential relationships between the diving behaviour and local environmental conditions by calculating Pearson correlation coefficients between the depth of the ascent rate change for each dive and, separately, the depth of the local OMZ, the depth of the 2.5 ml l^{-1} DO isopleth, time spent below 100 m (i.e. below the mixed layer), maximum depth of the dive, time spent in waters cooler than 18°C, and the depth of 18°C isotherm. 18°C was chosen as the temperature threshold for these analyses since the silvertip sharks spent >98% of their time in waters warmer than this temperature (Table 2). A DO level of 2.5 ml l^{-1} was assumed as a threshold for respiratory stress in a species like the silvertip shark based on levels reported in the literature for active ram-ventilating shark species, including

412 mako sharks (*Isurus oxyrhinchus*, Vetter et al. 2008), bonnethead (*Sphyrna tiburo*), and
413 blacknose sharks (*Carcharhinus acronotus*, Carlson & Parsons 2001). We estimated the depth
414 of the upper bound of the local oxygen minimum zone (OMZ) at each dive location by
415 analysing the gradient of the DO-depth curve, assuming that DO declines relatively steeply
416 from the surface to the start of the OMZ but stabilises at that depth (Sewell & Fage 1948).

417 To better visualise the relationships between average DO and temperature profiles across
418 dives, and the depth of the transition points, we calculated the mean (± CI) temperature and
419 estimated DO at 10 m intervals across all dives, and plotted this against depth. We then
420 superimposed on the depth axis the mean, CI and IQR of the transition point depths.

421 We also investigated whether the depth at which changes in ascent rate occurred was
422 associated with rates of increase in DO levels, rather than absolute values. For each dive's
423 ascent phase we calculated the ascent rate (m s^{-1}) at each recorded 15 s time interval, based
424 on the depth change since the previous depth-time record, and the corresponding vertical
425 rate of change in DO concentration, in ml per litre per metre of ascent. We pooled these data
426 for all dives and calculated the mean vertical ascent rate (± CI) for rates of change in DO
427 concentration of < -0.01 ml l^{-1} m^{-1}, -0.01 to +0.01 ml l^{-1} m^{-1}, +0.01 to +0.03 ml l^{-1} m^{-1}, and >
428 +0.03 ml l^{-1} m^{-1}.

3. Results

3.1. Overview of tag deployments

Seven silvertip sharks between 145 cm and 185 cm total length (mean = 158.4 ± 10.0 CI) were tagged with PATs between 12 February 2013 and 27 March 2014 (Table 1). At total of 770 daily data records were obtained from the seven tags (mean = 126 ± 20 days, range = 101 to 180 days, Table 4.1). Two satellite tags released at their pre-programmed time (120 and 180 days after deployment); the remaining five tags released prematurely between 101 and 127 days after deployment (49-71% of the programmed time, Table 4.1). The maximum depth (± measurement error) recorded on these tags ranged from 328 ± 4 m to 792 ± 4 m (Table 1).

3.2. Horizontal movements of the sharks based on geolocation estimates

The geolocation-based position estimates indicate that it is unlikely that any of the tagged sharks left the BIOT MPA, with the daily location estimates for each tag suggesting that the sharks spent most of their time close to the Chagos Archipelago reef system (Figure 1c). However, care should be taken in interpreting the track information, as the 95% confidence intervals for each shark's daily position estimates were very large relative to the estimated distances moved by the sharks (Figure 1c), indicating the low precision for the position estimates. A preliminary investigation of geolocation errors relative to position fixes from passive acoustic telemetry is reported in the Supplementary Material.

3.3. Variation in the median depth and ambient water temperature occupied by silvertip sharks

Daily median depth for all tagged sharks ranged from 4.0 to 77.2 m (mean 36.5 ± 0.84 m). The median daily depth for each tagged shark matched the contours of the relatively warm surface mixed layer (Figure 2a-g), with sharks spending 50% of their time in the lower part of the mixed layer (Figure 2a-g). The Pearson correlation score between shark median daily depths and the mixed layer depth, pooled for all tags, was 0.77 (Figure 2h), and the relationship between shark median depth and mixed layer depth appeared consistent across tags and years (Figure 3a). Daily mixed layer depth ranged from 18 m to 98 m. Mixed layer

456 depth was shallowest in May (median 38 m, 95% range 24 – 51 m) and deepest in August
457 (median 82 m, 95% range 68 – 90 m, Figure 3a).

458 There was significant monthly variation in the sharks' median depth (Figure 3a; Welch's
459 ANOVA $F_{6,764}$ = 134.3 , p <0.001), with post-hoc tests showing that sharks moved shallower in
460 April, May and June than in February, July and August (Supplementary Table S4), as the MLD
461 shoaled (Figure 3a). In contrast, the daily median water temperature occupied by sharks
462 varied comparatively little. Daily median temperature averaged 27.2 ± 0.1°C overall (range
463 26.8 to 27.6°C, Figure 3b). Local SST, in contrast, varied by up to 3°C during the deployment
464 periods (Figure 3b).

465 The median depth occupied by the sharks varied on shorter timescales between day and night
466 and between lunar phases at night time (Figure 4). Analysis of variance found significant
467 effects of time of day ($F_{1,954}$= 454.16, p < 0.001), lunar phase ($F_{3,954}$ = 7.28, p < 0.001) and the
468 interaction between time of day and lunar phase ($F_{3,954}$ = 10.63, p < 0.001). Analysis of
469 between-group differences using Tukey's test showed that sharks were significantly deeper
470 during daylight overall, by ~11 m, and night-time depths were greater by up to 6.1 m when
471 there was a full moon (Figure 4, Supplementary Table S5).

472 **3.4. Time below depth and temperature thresholds**

473 The sharks in the study spent an average of 5.1 ± 0.5% of their monitored time below 75 m,
474 1.5 ± 0.1 % below 100 m and only and 0.3 ± 0.1 % of their time (<5 minutes per day) below
475 150 m. Time spent below 100 m was significantly higher during day time ($t_{559.63}$ = -3.56, p <
476 0.001), consistent with day/night patterns in median depth, but sharks spent more time
477 below 150 m during the night ($t_{757.64}$ = -3.01, p = 0.002; Table 2). Sharks spent 14% of their
478 time in waters between 22 °C and 25 °C, i.e. up to 5 °C cooler than their median ambient
479 temperature, but only 1% of their time (~ 14 minutes per day) in water cooler than 18°C (Table
480 2). Over 99% of the shark's time was therefore spent in depths shallower than 150 m and
481 warmer than 18 °C.

3.5. Modelling of shark median depth against environmental variables

Generalised Linear Mixed Models were used to determine the influence of mixed layer depth, time of day (TOD), lunar phase (Moon), SST, and shark total length on the sharks' semi-diel (i.e., day vs night) median depth. Tag ID was included as a random factor, along with a second-order autoregressive term to account for autocorrelation in the time series data (Supplementary Figure S4). The six best models had similar AICc values, between 6335.2 and 6339.1 (Table 3, Supplementary Table S6), with the model with the lowest AIC including MLD, TOD and TL as fixed predictors. Diagnostics plots did not reveal any issues with model residuals (Supplementary Figure S7). The most parsimonious model included just MLD and TOD as predictors, with a model AICc only slightly higher than best performing model. However, marginal R^2 (R^2m), indicating variance explained by the fixed predictors, was improved from 0.27, for this base model, to 0.32 by the addition of TL, and 0.34 for models including a TOD*Moon interaction as well as TL (Table 3), indicating that the addition of both TL and the lunar variable explained additional variation in the data. Sea surface temperature appeared to make only a small contribution to improving model R^2m for the associated increase in AICc. Marginal and conditional R^2 values were similar for all models (Supplementary Table S6), indicating that random effect of Tag ID made a relatively small contribution to explained variance. Effect sizes for the fixed predictors were consistent across models. Predicted depth increased by ~3 m for every 10 m increase in MLD and, on average, ~10 m during daylight (Table 3). The influence of SST as an environmental factor was smaller (0.7-0.8 m increase in depth per 1°C SST), and standardised effect sizes for MLD and SST (0.29 vs 0.04, Table 3) show that MLD exerts a much larger influence on shark depth than variations in SST. For the models including the interaction between TOD and lunar phase, shark depth ~5.5 m deeper on nights with a full moon, relative to nights of the new moon (Table 3). Large individuals were predicted to occupy deeper depths, with predicted median depth increasing ~1.5 m for each 10 cm increase in total length.

3.6. Diving behaviour

The tag recovered with the full archival time series data set (Tag 1, ID 391300800, Table 1) contained records of 61 dives below 200 m, averaging one every three days. Dives were typically short in duration, averaging 5.3 ± 0.7 minutes, with a steady descent to 'target' depth

and a rapid ascent from depth (Supplementary Figures S8a, S8b). On returning from dives below 200 m the vertical ascent rate decreased sharply between 200 m and 100 m depth (Supplementary Figure S8a,b). Mean vertical ascent rates before and after this transition point in the ascent were 0.59 ± 0.05 ms^{-1} and 0.12 ± 0.01 ms^{-1}, respectively, a mean reduction of 80% (Welch t-test: $t_{71.5}$ = 19.892, $p < 0.001$). The change in ascent rate occurred at an average depth of 121.3 ± 7.2 m (IQR 103.5 – 138.0 m). The correlations between the depth of the transition point in the ascent rate and the depths of the upper boundary of the OMZ and the 2.5 ml l^{-1} DO isopleth on individual dives were 0.35 (t_{60}= 2.887, p = 0.005) and 0.32 (t_{60} = 2.625, p = 0.01), respectively, both stronger than the correlations between transition point depth and other environmental or dive parameters, such as temperature or maximum dive depth, although the differences are small (Supplementary Table S7). However, visual comparison of mean transition point depth and the average DO and temperature profiles of the dives also suggested that the point at which ascent rate slowed was more strongly associated with increasing oxygen levels at the upper boundary of the oxygen minimum zone, rather than abrupt changes in temperature (Figure 5, Supplementary Figure S5c,d). The shark's vertical ascent rate slowed as DO concentration began to increase at > 0.03 $ml.l^{-1}$ per metre of ascent, i.e. when the shark had reached increasingly oxygen-rich depths (Supplementary Figure S9).

4. Discussion

Using data from seven pop-up satellite tags, we modelled the vertical movements of silvertip sharks around the Chagos Archipelago in the BIOT MPA . While the sample size was small, the tagged sharks exhibited consistent and predictable vertical space use with respect to environmental drivers, suggesting that at our findings may be more widely generalisable. Water column thermal structure appeared a key driver of overall depth use, with the sharks following seasonal variations in the thermal contours of the mixed layer and occupying a relatively narrow temperature band similar to that reported elsewhere (Bond et al. 2015). Depth use varied predictably at shorter time scales, deeper during daylight and on nights of the full moon, and increased with the size of the tagged individuals, consistent with observations of diel vertical migration and ontogenetic variation in depth range in other

ectothermic predators. There was also some evidence, albeit limited to a single tag, that the sharks' diving behaviour is influenced by dissolved oxygen (DO) levels in the water column.

4.1. Temperature and light as predictors of vertical space use in silvertip sharks

Variation in silvertip sharks' daily median depth was strongly linked to the changing depth of the mixed layer over the study period, but despite the daily median depth of the seven sharks varying by over 50 m, tags recorded a consistent median ambient temperature of around 27°C. The animals' changing focal depth appears related to variations in the temperature gradient within the mixed layer, which altered the depth at which their 'Goldilocks zone' was located (i.e. the depth that the water temperature was 'just right'). Median daily water temperature recorded by tags on silvertip sharks in BIOT is similar to the 26.3°C average recorded by Bond et al. (2015) for an individual in Fiji, suggesting consistency in silvertip sharks' thermal preference across locations. While Espinoza et al. (2015a) did not directly measure ambient water temperature for silvertips sharks tagged on the GBR, they proposed behavioural thermoregulation (a 'hunt warm, rest cool' strategy) as an explanation for diel variation in depth use, and consequently the detection patterns observed in their passive telemetry study. Thermoregulation is proposed as a key driver in the vertical movements of several endothermic shark species, including blue (Campana et al. 2011), whale (Thums et al. 2013), blacktip reef (Speed et al. 2012) and leopard sharks (*Triakis semifasciata*, Hight and Lowe, 2007), and appears to be a driver of vertical space use in other ectothermic taxa around the Chagos Archipelago. Curnick et al. (2020) found that silky sharks tagged around the Chagos Archipelago spent the majority of their time in the top 100 m, in water from 24°C to 30°C. Andrzejaczek et al. (2020) obtained similar results from PAT deployments on reef manta rays (*Manta alfredi*) in the same location, finding that reef mantas spent most time within the mixed layer between 25-50 m, with a median temperature of 27.3 °C.

While water column thermal structure predicted the sharks' *average* depth, shorter term variations in depth were predicted by time of day in combination with lunar phases, suggesting that silvertip sharks engage in light-based diel vertical migration, as seen in pelagic species such as blue (Campana et al. 2011) and bigeye thresher sharks (*Alopias superciliosus*, Coelho et al. 2015). Espinoza et al. (2015a) hypothesised that silvertip sharks on the GBR 'rested' in deep channels between reefs during the day, before hunting in the shallows around

571 on reefs at night, and Bond et al. (2015) reported that a silvertip shark tagged with a satellite
572 tag had a significantly deeper mean depth during daytime than at night. Depth histograms
573 reported in that study suggest a median daytime depth of ~70 m, vs ~30 m at night (Bond et
574 al. 2015, p5). Baited camera surveys of reef associated sharks in the Chagos Archipelago also
575 found silvertip sharks were more abundant at depth of 70-80 m than on shallow reef sites
576 during daytime (Tickler et al. 2015). Vertical movements synchronised with diel and lunar
577 cycles have also been observed on reefs in Palau for grey reef sharks, a close congener (Vianna
578 et al. 2013). While thermoregulation might also be a driver of short-term vertical movements
579 by silvertip sharks in the BIOT, as hypothesised by Espinoza et al. (2015a), the fact that their
580 vertical space use also varies with changes in moon phase (i.e., light levels) at night suggests
581 light as primary driver, potentially mediated by the light-driven vertical migration of prey
582 species. Diet and stable isotope-based studies suggest silvertip sharks exploit a high
583 percentage of pelagic prey resources (Cortés 1999, Curnick et al. 2019). In the BIOT, where
584 the outer reefs of atolls abut deep pelagic waters (1000 – 3000 m), light-driven diel vertical
585 migration may bring pelagic prey into the surface waters adjacent to the reefs at night,
586 drawing predators like silvertip sharks. Curnick et al. (2020) and Andrzejaczek et al. (2020)
587 found that silky sharks and reef mantas both exhibited diel vertical migration near reefs in
588 the BIOT, with the latter study hypothesising that reef mantas exploited vertically migrating
589 mesopelagic zooplankton in offshore surface waters at night. Together, these results suggest
590 that temperature and light levels may be fundamental drivers of vertical space use of large
591 ectothermic predators around reefs, driving similar patterns in space use across disparate
592 taxa.

593 **4.2. Diving behaviour**

594 Silvertip sharks spent > 98% of their time in the top 100 m of the water column, but dives to
595 almost 800 m were recorded, approaching the maximum depth reported for this species
596 (Compagno 1984). Data from a single tag showed that dives below 200 m were short (~5
597 minutes) and relatively infrequent. Purposes for these dives might include predator
598 avoidance, thermoregulation and foraging (Howey et al. 2016, Andrzejaczek et al. 2020, Royer
599 et al. 2023). Predator avoidance cannot be discounted, given the presence in the BIOT of large
600 shark species like shortfin mako, *Isurus oxyrinchus* (Forrest 2019), and hammerhead sharks,
601 Sphyrnidae (Tickler et al. 2017), that prey on smaller sharks, but silvertip sharks might be

602 expected to take refuge on the reefs in BIOT, rather than dive to extreme depths.
603 Thermoregulation, seeking cooler water temperatures, also seems as unlikely motivation for
604 deep diving as the water temperature drops below 20°C at relatively shallow depths of ~100
605 m, beneath the mixed layer (Hosegood et al. 2019). Foraging may therefore be the most
606 parsimonious explanation. Periodic deep dives are hypothesised to provide opportunities to
607 pelagic sharks, including oceanic white tip (Howey et al. 2016), blue (Braun et al. 2019) and
608 scalloped hammerhead sharks (*Sphyrna lewini*, Royer et al. 2023), to encounter slow-moving
609 mesopelagic prey. Silvertip sharks, which are known to exploit pelagic prey in the BIOT
610 (Curnick et al. 2019), may employ similar strategies. Previous studies have suggested that reef
611 shark foraging behaviour horizontally connects pelagic and reef ecosystems (McCauley et al.
612 2012, Williams et al. 2018). By foraging at depth, silvertip sharks may also be contributing to
613 coupling deep pelagic and shallow reef ecosystems in the BIOT.

614 Dissolved oxygen concentration is thought to influence the vertical space use and diving
615 behaviour of several marine predators including billfish and tunas (Prince & Goodyear 2006,
616 Prince et al. 2010, Carlisle et al. 2016, Pohlot & Ehrhardt 2017) and mako sharks (Vetter et al.
617 2008, Abascal et al. 2011), and analysis of the individual dive trajectories of one shark found
618 possible evidence of an influence of dissolved oxygen availability on the vertical space use of
619 silvertip sharks. Mesopelagic dives, identified in the high-resolution depth and temperature
620 data from a physically-recovered tag, were characterised by a rapid and constant rate of
621 descent, a period of assumed foraging, and a return to surface waters in two distinct ascent
622 rate phases. These 'transition point' dives (*sensu* Howey et al. 2016), were characterised by a
623 50-80% reduction in vertical ascent rate, occurring at a fairly consistent depth. Howey et al.
624 (2016) observed a similar pattern in dives by oceanic whitetip sharks in the Bahamas and,
625 though they lacked *in situ* oxygen measurements to explore further, hypothesised that this
626 behaviour might coincide with the sharks moving out of the oxygen minimum zone after
627 mesopelagic dives. We used DO levels inferred from climatological datasets and the
628 estimated positions of the tag, meaning results are preliminary, but found that transition
629 point depths were more strongly correlated with the estimated upper bound of the local OMZ
630 (i.e., DO levels are consistently below 2.5 ml l^{-1}) than with changes in water temperature,
631 which showed no distinct features at the depth of the ascent rate change. Under this oxygen-
632 limitation hypothesis, the rapid portion of the silvertip shark's ascent from dives within the

OMZ is designed to minimise continued exposure to low dissolved oxygen levels and/or increase ram breathing efficiency, while the sudden deceleration reduces energy expenditure once better-oxygenated waters are reached. A recent study on billfish found that individuals exhibited rapid swimming speeds immediately after capture and release by sports-fishers, a behaviour hypothesised to reduce high lactate levels accumulated during capture (Logan et al. 2022). Rapid ascents after time spent in low oxygen waters may serve a similar function for silvertip sharks. An interesting alternate hypothesis, derived from a more sophisticated biologging study, is that transition point dive profiles in ectothermic sharks relate to 'breath hold' behaviour used to minimise heat loss via the gills during deep, cold dives (Royer et al. 2023). Royer et al. (2023) observed that body temperature in scalloped hammerheads tagged with intra-muscular temperature probes did not fall as expected during the deepest parts of dives, when the water temperature was < 10°C. They hypothesised that the sharks were reducing ram-ventilation during 'sprint' descents and foraging at depth, but abruptly slowed their swimming rate (measured with tail beat telemetry) once normal respiration recommenced partway through their ascent, at which point their body temperature started to fall quickly. Dive profiles presented in that paper are very similar to those we observed (Supplementary figure S8), suggesting that body temperature management may also explain silvertip dive profiles. The correlation between oxygen levels and transition point depth may be explained by the fact that sharks engaging in breath hold thermoregulation (Royer et al. 2023) don't restart regular ram ventilation until they are back in relatively well-oxygenated water. *In situ* measurement of oxygen, using DO sensor tags (Coffey & Holland 2015), and intra-muscular probes and accelerometery as used by Royer et al. would help explore this question further.

4.3. Vertical space use, management and conservation

Species' horizontal space use is often considered when evaluating their exposure to fisheries (Queiroz et al. 2019, Jacoby et al. 2020) and the efficacy of MPAs (Dwyer et al. 2020). However, vertical space use also has important management implications, and predictable vertical movements by silvertip sharks may increase their vulnerability to fishing, but also be used to tailor enforcement activities to periods of greatest risk. The silvertip shark's core depth range in the BIOT MPA overlaps with the relatively shallow (30-100 m depth) longlines

set by regional fishing fleets (Aneesh et al. 2016, Hewapathirana & Gunawardane 2017), some of whom are known to illegally fish in BIOT (Martin et al. 2013, Tickler et al. 2019). Jacoby et al. (2020) found that silvertip sharks' wider movements around the Chagos Archipelago increased their exposure to illegal fishing activity; predictable vertical space use may increase their vulnerability by allowing fishers to target them based on simple environmental cues. Vianna et al. (2013) hypothesised a similar problem for grey reef sharks in Palau, which showed predictable depth changes correlated with diel and lunar cycles, and Andrzejaczek et al. (2020) noted that reef mantas in BIOT occupied a predictable depth range which might increase their vulnerability to fishing gears. Our study's deployment period was focussed on the March to July period in BIOT and so missed the peak fishing season for pelagic fisheries targeting tunas and seasonal offshore productivity peaks. Longer tag release times would help fill the gap in our understanding of shark movements and fisheries exposure.

A preference for relatively cool waters and an apparent intolerance to low-DO conditions may have longer-term implications for silvertip sharks, particularly in remote locations like the BIOT with limited connectivity to other reef systems. Climate change is leading to warming oceans (Cheung et al. 2016), changes in mixed layer depth (e.g. Jang et al. 2011, Mohan et al. 2021), shoaling and expanding OMZs (Gilly et al. 2013), and an overall reduction in DO in the ocean (Breitburg et al. 2018). Declining oxygen availability as oceans warm is expected to lead to a poleward shift in species' ranges (Cheung et al. 2009, Sunday et al. 2011, Robinson et al. 2015). The Chagos Archipelago is relatively isolated, however, and surrounded by water 4 km deep, making (southerly) poleward migration by its inhabitants difficult, if not impossible. Behavioural thermoregulation, i.e. moving to deeper, cooler water (Dulvy et al. 2008), may allow short-term adaptation to warming surface waters for species like silvertip sharks. However, continued surface warming, estimated at 0.11°C per decade globally and 0.15°C per decade in the Indian Ocean (Roxy et al. 2020), may interact synergistically with changing oxygen availability to constrain their available vertical habitat. Shoaling of OMZs (Stramma et al. 2012, Gilly et al. 2013) and mixed layer depth (Jang et al. 2011, Mohan et al. 2021) may push species like silvertip sharks towards the surface, while warming surface waters compress their thermal niche from above. As well the physiological strain, this may also increase silvertips sharks' vulnerability to fishing by making their vertical space use more constrained and predictable. Climate change is forecast to have important impacts on fish stocks (e.g.

Cheung et al. 2016), and our study suggests that important non-target species like reef sharks may also be affected in terms of both physiological fitness and increasing restrictions to their useable habitat. Reducing direct anthropological pressures on reef sharks and their habitats, e.g., through well-enforced MPAs, may help maintain biodiversity and enhance species' resilience to environmental change (Dulvy 2006, Edgar et al. 2014, Davies et al. 2017), but tackling the root causes of the warming will be necessary to avert longer term impacts.

4.4. Conclusion

Human fishing impacts on reef sharks are of ongoing concern and the relatively restricted and predictable vertical niche of species like silvertip sharks may accentuate their vulnerability, even in nominally protected areas (Bradley et al. 2019, Tickler et al. 2019, Collins et al. 2021). Moving closer to the surface at night may increase their exposure to illegal fishing when detection and enforcement are most difficult. Enforcement reports by the BIOT authorities include accounts of vessels being encountered at dawn with their fishing gear already deployed (e.g., IOTC Secretariat 2015), suggesting that night-time fishing is already the norm for those fishing illegally in BIOT. Combining vertical spatial ecology with data on horizontal space use allows managers of both fisheries and protected areas to predict the times and locations of greatest vulnerability to fishing for particular species, to better prioritise enforcement efforts, and to potentially regulate fishing activity to avoid bycatch of species of concern, as has been attempted with gillnet depths to avoid cetacean bycatch (Kiszka et al. 2018).

In addition to helping predict the spatial overlap of species like silvertip sharks with fishing activities, archival tags, including newer designs fitted with additional environmental sensors (Coffey & Holland 2015), may allow us to model the responses of sharks and other taxa as the ocean warms and temperature and oxygen availability change both horizontally and vertically (Cheung et al. 2009, Gilly et al. 2013). Refining our understanding of the physiological constraints of taxa, and their vulnerability and likely responses to ocean warming and deoxygenation, will be vital to managing the future ocean. While acoustic telemetry is typically considered a more cost-effective option for the study of reef-associated shark species (Whoriskey & Hindell 2016, but see Bond et al. 2015, Andrzejaczek et al. 2020, Bradley et al. 2019), our study provides further evidence that satellite archival tags can reveal valuable

724 insights into their spatial ecology, expanding our knowledge of the vertical dimension of shark
725 ecology (Andrzejaczek et al. 2022).

726 Acknowledgements

727 Field work was completed under research approvals from the United Kingdom Foreign and
728 Commonwealth Office with the support of the Bertarelli Foundation Programme in Marine
729 Science. Animal handling procedures were approved by the Stanford University
730 Administrative Panel on Laboratory Animal Care under permit APLAC-10765, held by the
731 Block Laboratory at Hopkins Marine Station, and the Zoological Society of London's animal
732 ethics committee.

733 D.T analysed the data and drafted the manuscript, with reviews and editorial input from all
734 co-authors. D.T., A.C., T.C., R.S., D.C. and J.D. collected the field data. D.T. and A.C. conceived
735 the paper, with analytical support from T.C. and J.D. J.M. provided advice on statistics and
736 manuscript structure and editing. B.B provided project resources and editorial input.
737 Additional comments on the MS were received from Professor Dirk Zeller at the Sea Around
738 Us – Indian Ocean and UWA Oceans Institute.

References

Abascal FJ, Quintans M, Ramos-Cartelle A, Mejuto J (2011) Movements and environmental preferences of the shortfin mako, *Isurus oxyrinchus*, in the southeastern Pacific Ocean. Mar. Biol. 158:1175–1184.

Afonso AS, Hazin FHV (2015) Vertical movement patterns and ontogenetic niche expansion in the tiger shark, *Galeocerdo cuvier*. PLOS ONE 10:e0116720.

Akima H (1978) A Method of Bivariate Interpolation and Smooth Surface Fitting for Irregularly Distributed Data Points. ACM Trans. Math. Software 4:148–159.

Andrzejaczek S, Chapple T, Curnick D, Carlisle A, Castleton M, Jacoby D, Peel L, Schallert R, Tickler D, Block B (2020) Individual variation in residency and regional movements of reef manta rays *Mobula alfredi* in a large marine protected area. Mar. Ecol. Prog. Ser. 639:137–153.

Andrzejaczek S, Gleiss AC, Jordan LKB, Pattiaratchi CB, Howey LA, Brooks EJ, Meekan MG (2018) Temperature and the vertical movements of oceanic whitetip sharks, *Carcharhinus longimanus*. Sci Rep 8:8351.

Andrzejaczek S, Gleiss AC, Pattiaratchi CB, Meekan MG (2019) Patterns and drivers of vertical movements of the large fishes of the epipelagic. Rev. Fish Biol. Fish. 29:335–354.

Andrzejaczek S, Lucas TCD, Goodman MC, Hussey NE, Armstrong AJ, Carlisle A, Coffey DM, Gleiss AC, Huveneers C, Jacoby DMP, Meekan MG, Mourier J, Peel LR, Abrantes K, Afonso AS, Ajemian MJ, Anderson BN, Anderson SD, Araujo G, Armstrong AO, Bach P, Barnett A, Bennett MB, Bezerra NA, Bonfil R, Boustany AM, Bowlby HD, Branco I, Braun CD, Brooks EJ, Brown J, Burke PJ, Butcher P, Castleton M, Chapple TK, Chateau O, Clarke M, Coelho R, Cortes E, Couturier LIE, Cowley PD, Croll DA, Cuevas JM, Curtis TH, Dagorn L, Dale JJ, Daly R, Dewar H, Doherty PD, Domingo A, Dove ADM, Drew M, Dudgeon CL, Duffy CAJ, Elliott RG, Ellis JR, Erdmann MV, Farrugia TJ, Ferreira LC, Ferretti F, Filmalter JD, Finucci B, Fischer C, Fitzpatrick R, Forget F, Forsberg K, Francis MP, Franks BR, Gallagher AJ, Galvan-Magana F, García ML, Gaston TF, Gillanders BM, Gollock MJ, Green JR, Green S, Griffiths CA, Hammerschlag N, Hasan A, Hawkes LA, Hazin F, Heard M, Hearn A, Hedges KJ, Henderson SM, Holdsworth J, Holland

767 KN, Howey LA, Hueter RE, Humphries NE, Hutchinson M, Jaine FRA, Jorgensen SJ, Kanive PE,
768 Labaja J, Lana FO, Lassauce H, Lipscombe RS, Llewellyn F, Macena BCL, Mambrasar R,
769 McAllister JD, Phillips SRM, McGregor F, McMillan MN, McNaughton LM, Mendonça SA,
770 Meyer CG, Meyers M, Mohan JA, Montgomery JC, Mucientes G, Musyl MK, Nasby-Lucas N,
771 Natanson LJ, O'Sullivan JB, Oliveira P, Papastamtiou YP, Patterson TA, Pierce SJ, Queiroz N,
772 Radford CA, Richardson AJ, Richardson AJ, Righton D, Rohner CA, Royer MA, Saunders RA,
773 Schaber M, Schallert RJ, Scholl MC, Seitz AC, Semmens JM, Setyawan E, Shea BD, Shidqi RA,
774 Shillinger GL, Shipley ON, Shivji MS, Sianipar AB, Silva JF, Sims DW, Skomal GB, Sousa LL,
775 Southall EJ, Spaet JLY, Stehfest KM, Stevens G, Stewart JD, Sulikowski JA, Syakurachman I,
776 Thorrold SR, Thums M, Tickler D, Tolloti MT, Townsend KA, Travassos P, Tyminski JP, Vaudo
777 JJ, Veras D, Wantiez L, Weber SB, Wells RJD, Weng KC, Wetherbee BM, Williamson JE, Witt
778 MJ, Wright S, Zilliacus K, Block BA, Curnick DJ (2022) Diving into the vertical dimension of
779 elasmobranch movement ecology. Sci. Adv. 8:eabo1754

780 Aneesh KK, Pravin P, Khanolkar P, Baiju M, Meenakumari B (2016) The effect of depth of
781 operation and soaking time on catch rates in the experimental tuna longline fisheries in
782 Lakshadweep Sea, India. Iran. J. Fish. Sci. 15:597–605.

783 Araujo G, Agustines A, Tracey B, Snow S, Labaja J, Ponzo A (2019) Photo-ID and telemetry
784 highlight a global whale shark hotspot in Palawan, Philippines. Sci. Rep. 9:17209.

785 Bartoń K (2022) MuMIn: Multi-Model Inference. R package version 1.46.0. https://CRAN.R-
786 project.org/package=MuMIn

787 Baum JK, Myers RA (2004) Shifting baselines and the decline of pelagic sharks in the Gulf of
788 Mexico. Ecol. Lett. 7:135–145.

789 Baumgartner MF, Lysiak N, Schuman C, Urban-Rich J, Wenzel FW (2011) Diel vertical
790 migration behavior of *Calanus finmarchicus* and its influence on right and sei whale
791 occurrence. Mar. Ecol. Prog. Ser. 423:167–184.

792 Block BA, Jonsen ID, Jorgensen SJ, Winship AJ, Shaffer SA, Bograd SJ, Hazen EL, Foley DG,
793 Breed GA, Harrison AL, Ganong JE, Swithenbank A, Castleton M, Dewar H, Mate BR, Shillinger

794 GL, Schaefer KM, Benson SR, Weise MJ, Henry RW, Costa DP (2011) Tracking apex marine
795 predator movements in a dynamic ocean. Nature 475:86–90.

796 Bond ME, Tolentino E, Mangubhai S, Howey LA (2015) Vertical and horizontal movements of
797 a silvertip shark (*Carcharhinus albimarginatus*) in the Fijian archipelago. Anim. Biotelemetry
798 3:19.

799 Bost CA, Zorn T, Le Maho Y, Duhamel G (2002) Feeding of diving predators and diel vertical
800 migration of prey: King penguin diet versus trawl sampling at Kerguelen Islands. Mar. Ecol.
801 Prog. Ser. 227:51–61.

802 Bradley D, Mayorga J, McCauley DJ, Cabral RB, Douglas P, Gaines SD (2019) Leveraging
803 satellite technology to create true shark sanctuaries. Conserv. Lett. 12:e12610.

804 Braun CD, Gaube P, Sinclair-Taylor TH, Skomal GB, Thorrold SR (2019) Mesoscale eddies
805 release pelagic sharks from thermal constraints to foraging in the ocean twilight zone. PNAS
806 116:17187–17192.

807 Braun CD, Skomal GB, Thorrold SR, Berumen ML (2014) Diving Behavior of the Reef Manta
808 Ray Links Coral Reefs with Adjacent Deep Pelagic Habitats. PLOS ONE 9:e88170.

809 Breheny P, Burchett W (2017) Visualization of Regression Models Using visreg. The R Journal
810 9:56–71.

811 Breitburg D, Levin LA, Oschlies A, Grégoire M, Chavez FP, Conley DJ, Garçon V, Gilbert D,
812 Gutiérrez D, Isensee K, Jacinto GS, Limburg KE, Montes I, Naqvi SWA, Pitcher GC, Rabalais NN,
813 Roman MR, Rose KA, Seibel BA, Telszewski M, Yasuhara M, Zhang J (2018) Declining oxygen
814 in the global ocean and coastal waters. Science 359:eaam7240.

815 Cagua EF, Cochran JEM, Rohner CA, Prebble CEM, Sinclair-Taylor TH, Pierce SJ, Berumen ML
816 (2015) Acoustic telemetry reveals cryptic residency of whale sharks. Biol. Lett. 11:20150092.

817 Campana SE, Dorey A, Fowler M, Joyce W, Wang Z, Wright D, Yashayaev I (2011) Migration
818 pathways, behavioural thermoregulation and overwintering grounds of blue sharks in the
819 Northwest Atlantic. PLOS ONE 6:e16854.

820 Carlisle AB, Kochevar RE, Arostegui MC, Ganong JE, Castleton M, Schratwieser J, Block BA
821 (2016) Influence of temperature and oxygen on the distribution of blue marlin (*Makaira*
822 *nigricans*) in the Central Pacific. Fish. Oceanogr. 26:34–48.

823 Carlisle AB, Litvin SY, Hazen EL, Madigan DJ, Goldman KJ, Lea RN, Block BA (2015)
824 Reconstructing habitat use by juvenile salmon sharks links upwelling to strandings in the
825 California Current. Mar. Ecol. Prog. Ser. 525:217–228.

826 Carlisle AB, Perle CR, Goldman KJ, Block BA (2011) Seasonal changes in depth distribution of
827 salmon sharks (*Lamna ditropis*) in Alaskan waters: implications for foraging ecology. Can. J.
828 Fish. Aquat. Sci. 68:1905–1921.

829 Carlisle AB, Tickler D, Dale JJ, Ferretti F, Curnick DJ, Chapple TK, Schallert RJ, Castleton M,
830 Block BA (2019) Estimating space use of mobile fishes in a large marine protected area with
831 methodological considerations in acoustic array design. Front. Mar. Sci. 6:256.

832 Carlson J (2003) Respiratory and hematological responses of the bonnethead shark, *Sphyrna*
833 *tiburo*, to acute changes in dissolved oxygen. J. Exp. Mar. Biol. Ecol. 294:15–26.

834 Carlson JK, Parsons GR (2001) The effects of hypoxia on three sympatric shark species:
835 Physiological and behavioral responses. Environ. Biol. Fish. 61:427–433.

836 Chapman DD, Pikitch EK, Babcock E, Shivji MS (2005) Marine reserve design and evaluation
837 using automated acoustic telemetry: a case-study involving coral reef-associated sharks in the
838 Mesoamerican Caribbean. Mar. Technol. Soc. J. 39:42–55.

839 Chapman DD, Pikitch EK, Babcock EA, Shivji MS (2007) Deep-diving and diel changes in vertical
840 habitat use by Caribbean reef sharks *Carcharhinus perezi*. Mar. Ecol. Prog. Ser. 344:271–275.

841 Cheung WWL, Lam VWY, Sarmiento JL, Kearney K, Watson R, Pauly D (2009) Projecting global
842 marine biodiversity impacts under climate change scenarios. Fish Fish. 10:235–251.

843 Cheung WWL, Reygondeau G, Frölicher TL (2016) Large benefits to marine fisheries of
844 meeting the 1.5°C global warming target. Science 354:1591–1594.

845 Chin A, Kyne PM, Walker TI, McAuley RB (2010) An integrated risk assessment for climate
846 change: analysing the vulnerability of sharks and rays on Australia's Great Barrier Reef. Global
847 Change Biol. 16:1936–1953.

848 Coelho R, Fernandez-Carvalho J, Santos MN (2015) Habitat use and diel vertical migration of
849 bigeye thresher shark: Overlap with pelagic longline fishing gear. Mar. Environ. Res. 112:91–
850 99.

851 Coffey DM, Holland KN (2015) First autonomous recording of *in situ* dissolved oxygen from
852 free-ranging fish. Anim. Biotelemetry 3:47.

853 Coffey DM, Royer MA, Meyer CG, Holland KN (2020) Diel patterns in swimming behavior of a
854 vertically migrating deepwater shark, the bluntnose sixgill (Hexanchus griseus). PLOS ONE
855 15:e0228253.

856 Collins C, Nuno A, Benaragama A, Broderick A, Wijesundara I, Wijetunge D, Letessier TB (2021)
857 Ocean-scale footprint of a highly mobile fishing fleet: Social-ecological drivers of fleet
858 behaviour and evidence of illegal fishing. People Nat. 3:740–755.

859 Compagno LJV (1984) Sharks of the world: An annotated and illustrated catalogue of shark
860 species known to date. The Food and Agriculture Organisation of the United Nations (FAO),
861 Rome, Italy. 654 p.

862 Cortés E (1999) Standardized diet compositions and trophic levels of sharks. ICES J. Mar. Sci.
863 56:707–717.

864 Curnick DJ, Carlisle AB, Gollock MJ, Schallert RJ, Hussey NE (2019) Evidence for dynamic
865 resource partitioning between two sympatric reef shark species within the British Indian
866 Ocean Territory. J. Fish Biol. 94:680–685.

867 Curnick DJ, Collen B, Koldewey HJ, Jones KE, Kemp KM, Ferretti F (2020) Interactions between
868 a large marine protected area, pelagic tuna and associated fisheries. Front. Mar. Sci. 7.318.

869 Curnick DJ, Andrzejaczek S, Jacoby DMP, Coffey DM, Carlisle AB, Chapple TK, Ferretti F,
870 Schallert RJ, White T, Block BA, Koldewey HJ, Collen B (2020) Behavior and Ecology of Silky

871 Sharks Around the Chagos Archipelago and Evidence of Indian Ocean Wide Movement. Front.
872 Mar. Sci. 7:596619.

873 Davies TE, Maxwell SM, Kaschner K, Garilao C, Ban NC (2017) Large marine protected areas
874 represent biodiversity now and under climate change. Sci. Rep. 7:9569.

875 Doherty PD, Baxter JM, Godley BJ, Graham RT, Hall G, Hall J, Hawkes LA, Henderson SM,
876 Johnson L, Speedie C, Witt MJ (2019) Seasonal changes in basking shark vertical space use in
877 the north-east Atlantic. Mar. Biol. 166:129.

878 Donaldson MR, Hinch SG, Suski CD, Fisk AT, Heupel MR, Cooke SJ (2014) Making connections
879 in aquatic ecosystems with acoustic telemetry monitoring. Front. Ecol. Environ. 12:565–573.

880 Dulvy NK (2006) Conservation biology: strict marine protected areas prevent reef shark
881 declines. Curr. Biol. 16:R989–R991.

882 Dulvy NK, Rogers SI, Jennings S, Stelzenmüller V, Dye SR, Skjoldal HR (2008) Climate change
883 and deepening of the North Sea fish assemblage: a biotic indicator of warming seas. J. Appl.
884 Ecol. 45:1029–1039.

885 Dunn N, Curnick D (2019) Using historical fisheries data to predict tuna distribution within the
886 British Indian Ocean Territory Marine Protected Area, and implications for its management.
887 Aquat. Conserv. Mar. Freshwater Ecosyst. 29:2057–2070.

888 Dwyer RG, Krueck NC, Udyawer V, Heupel MR, Chapman D, Pratt HL, Garla R, Simpfendorfer
889 CA (2020) Individual and population benefits of marine reserves for reef sharks. Curr. Biol.
890 30:480-489.e5.

891 Edgar GJ, Stuart-Smith RD, Willis TJ, Willis TJ, Kininmonth S, Kininmonth S, Baker SC, Baker SC,
892 Banks S, Banks S, Barrett NS, Becerro MA, Bernard ATF, Berkhout J, Buxton CD, Buxton CD,
893 Campbell SJ, Cooper AT, Cooper AT, Davey M, Davey M, Edgar SC, Försterra G, Försterra G,
894 Galván DE, Galván DE, Irigoyen AJ, Irigoyen AJ, Kushner DJ, Moura R, Parnell PE, Parnell PE,
895 Shears NT, Shears NT, Soler G, Strain EMA, Thomson RJ, Thomson RJ (2014) Global
896 conservation outcomes depend on marine protected areas with five key features. Nature
897 506:216–220.

898 Elith J, Leathwick JR, Hastie T (2008) A working guide to boosted regression trees. J. Anim.
899 Ecology 77:802–813.

900 Espinoza M, Gonzalez-Medina E, Dulvy NK, Pillans RD (2016) *Carcharhinus albimarginatus*.
901 The IUCN Red List of Threatened Species 2016: eT161526A68611084.

902 Espinoza M, Heupel MR, Tobin AJ, Simpfendorfer CA (2015a) Movement patterns of silvertip
903 sharks (*Carcharhinus albimarginatus*) on coral reefs. Coral Reefs 34:1–15.

904 Espinoza M, Lédée EJI, Simpfendorfer CA, Tobin AJ, Heupel MR (2015b) Contrasting
905 movements and connectivity of reef-associated sharks using acoustic telemetry: implications
906 for management. Ecol. Appl. 25:2101–2118.

907 Ferretti F, Worm B, Britten GL, Heithaus MR, Lotze HK (2010) Patterns and ecosystem
908 consequences of shark declines in the ocean. Ecol. Lett. 13:1055–1071.

909 Ferretti F, Curnick D, Liu K, Romanov EV, Block BA (2018) Shark baselines and the conservation
910 role of remote coral reef ecosystems. Sci. Adv. 4:eaaq0333.

911 Fisher JAD, Robert D, Le Bris A, Loher T (2017) Pop-up satellite archival tag (PSAT) temporal
912 data resolution affects interpretations of spawning behaviour of a commercially important
913 teleost. Anim. Biotelemetry 5:21.

914 Forrest JAH (2019) Pelagic ecology and solutions for a troubled ocean. PhD Thesis, University
915 of Western Australia, Perth, Western Australia.

916 Fox J, Monette G (1992) Generalized Collinearity Diagnostics. J. Am. Stat. Assoc. 87:178–183.

917 Francis MP, Holdsworth JC, Block BA (2015) Life in the open ocean: seasonal migration and
918 diel diving behaviour of Southern Hemisphere porbeagle sharks (*Lamna nasus*). Mar. Biol.
919 162:2305–2323.

920 Gilly WF, Beman JM, Litvin SY (2013) Oceanographic and biological effects of shoaling of the
921 oxygen minimum zone. Annu. Rev. Mar. Sci. 5:393–420.

922 Graham NAJ, Spalding MD, Sheppard CRC (2010) Reef shark declines in remote atolls highlight
923 the need for multi-faceted conservation action. Aquat. Conserv. Mar. Freshwater Ecosyst.
924 20:543–548.

925 Hammerschlag N, Gallagher AJ, Lazarre DM (2011) A review of shark satellite tagging studies.
926 J. Exp. Mar. Biol. Ecol. 398:1–8.

927 Haulsee DE, Fox DA, Breece MW, Clauss TM, Oliver MJ (2016) Implantation and Recovery of
928 Long-Term Archival Transceivers in a Migratory Shark with High Site Fidelity. PLOS ONE
929 11:e0148617

930 Hays GC, Koldewey HJ, Andrzejaczek S, Attrill MJ, Barley S, Bayley DTI, Benkwitt CE, Block B,
931 Schallert RJ, Carlisle AB, Carr P, Chapple TK, Collins C, Diaz C, Dunn N, Dunbar RB, Eager DS,
932 Engel J, Embling CB, Esteban N, Ferretti F, Foster NL, Freeman R, Gollock M, Graham NAJ,
933 Harris JL, Head CEI, Hosegood P, Howell KL, Hussey NE, Jacoby DMP, Jones R, Sannassy Pilly S,
934 Lange ID, Letessier TB, Levy E, Lindhart M, McDevitt-Irwin JM, Meekan M, Meeuwig JJ, Micheli
935 F, Mogg AOM, Mortimer JA, Mucciarone DA, Nicoll MA, Nuno A, Perry CT, Preston SG, Rattray
936 AJ, Robinson E, Roche RC, Schiele M, Sheehan EV, Sheppard A, Sheppard C, Smith AL, Soule B,
937 Spalding M, Stevens GMW, Steyaert M, Stiffel S, Taylor BM, Tickler D, Trevail AM, Trueba P,
938 Turner J, Votier S, Wilson B, Williams GJ, Williamson BJ, Williamson MJ, Wood H, Curnick DJ
939 (2020) A review of a decade of lessons from one of the world's largest MPAs: conservation
940 gains and key challenges. Mar. Biol. 167:159.

941 Heithaus MR, Wirsing AJ, Dill LM, Heithaus LI (2007) Long-term movements of tiger sharks
942 satellite-tagged in Shark Bay, Western Australia. Mar. Biol. 151:1455–1461.

943 Hewapathirana HPK, Gunawardane NDP (2017) Sri Lanka national report to the Scientific
944 Committee of the Indian Ocean Tuna Commission. Indian Ocean Tuna Commission, Victoria,
945 Seychelles.

946 Hight BV, Lowe CG (2007) Elevated body temperatures of adult female leopard sharks, Triakis
947 semifasciata, while aggregating in shallow nearshore embayments: Evidence for behavioral
948 thermoregulation? J Exp Mar Biol Ecol 352:114–128.

949 Hijmans RJ (2017) Geosphere: Spherical Trigonometry. R package version 1.5-7.
950 https://CRAN.R-project.org/package=geosphere

951 Hill RD, Braun MJ (2001) Geolocation by Light Level: The Next Step: Latitude. In: *Electronic*
952 *Tagging and Tracking in Marine Fisheries*. Reviews: Methods and Technologies in Fish Biology
953 and Fisheries, Sibert JR, Nielsen JL (eds) Springer Netherlands, Dordrecht, Netherlands., p
954 315–330

955 Hosegood PJ, Nimmo-Smith WAM, Proud R, Adams K, Brierley AS (2019) Internal lee waves
956 and baroclinic bores over a tropical seamount shark 'hot-spot.' Prog. Oceanogr. 172:34–50.

957 Howey LA, Tolentino ER, Papastamatiou YP, Brooks EJ, Abercrombie DL, Watanabe YY,
958 Williams S, Brooks A, Chapman DD, Jordan LKB (2016) Into the deep: the functionality of
959 mesopelagic excursions by an oceanic apex predator. Ecol. Evol. 6:5290–5304.

960 Howey-Jordan LA, Brooks EJ, Abercrombie DL, Jordan LKB, Brooks A, Williams S, Gospodarczyk
961 E, Chapman DD (2013) Complex movements, philopatry and expanded depth range of a
962 severely threatened pelagic shark, the oceanic whitetip (*Carcharhinus longimanus*) in the
963 western North Atlantic. PLOS ONE 8:e56588.

964 Hussey NE, Kessel ST, Aarestrup K, Cooke SJ, Cowley PD, Fisk AT, Harcourt RG, Holland KN,
965 Iverson SJ, Kocik JF, Flemming JEM, Whoriskey FG (2015) Aquatic animal telemetry: A
966 panoramic window into the underwater world. Science 348:1255642.

967 IOTC Secretariat (2015) IUU Provisional List for 2015.
968 http://iotc.org/sites/default/files/documents/2015/04/AllEF_20150413.pdf (accessed
969 March 14, 2016)

970 Jacoby DMP, Ferretti F, Freeman R, Carlisle AB, Chapple TK, Curnick DJ, Dale JJ, Schallert RJ,
971 Tickler D, Block BA (2020) Shark movement strategies influence poaching risk and can guide
972 enforcement decisions in a large, remote marine protected area. J. Appl. Ecol. 57:1782–1792.

973 Jang CJ, Park J, Park T, Yoo S (2011) Response of the ocean mixed layer depth to global
974 warming and its impact on primary production: a case for the North Pacific Ocean. ICES J. Mar.
975 Sci. 68:996–1007.

976 Jorgensen SJ, Chapple TK, Anderson SD, Hoyos M, Reeb CA, Block BA (2012)
977 Connectivity among White Sharks Coastal Aggregation Areas in the Northeastern Pacific. In:
978 *Global Perspectives on the Biology and Life History of the White Shark*. Domeier ML (ed) CRC
979 Press, Boca Raton, FL, p 159–168

980 Kara AB, Rochford PA, Hurlburt HE (2000) An Optimal Definition for Ocean Mixed Layer Depth.
981 J. Geophys. Res. Oceans. 105:16803–16821.

982 Kessel ST, Cooke SJ, Heupel MR, Hussey NE, Simpfendorfer CA, Vagle S, Fisk AT (2014) A review
983 of detection range testing in aquatic passive acoustic telemetry studies. Rev. Fish Biol. Fish.
984 24:199–218.

985 Kessel ST, Hussey NE (2015) Tonic immobility as an anaesthetic for elasmobranchs during
986 surgical implantation procedures. Can. J. Fish. Aquat. Sci. 72:1287–1291.

987 Kiszka JJ, Moazzam M, Nivière M, Shahid U, Khan B, Nawaz R (2018) Cetaceans in the tuna
988 drift gillnet fishery off Pakistan (Arabian Sea): can we reduce bycatch at low cost with no
989 impact on targeted species catch rates. In: *14th meeting of the IOTC Working Party on*
990 *Ecosystem and Bycatch, Cape Town, South Africa*. Indian Ocean Tuna Commission, Victoria,
991 Seychelles, p 10–14

992 Knip DM, Heupel MR (2010) Sharks in nearshore environments: models, importance, and
993 consequences. Mar. Ecol. Prog. Ser. 402:1–11.

994 Lazaridis E (2014) Lunar: Lunar Phase & Distance, Seasons and Other Environmental Factors
995 (Version 0.1-04). http://statistics.lazaridis.eu

996 Lea JSE, Humphries NE, von Brandis RG, Clarke CR, Sims DW (2016) Acoustic telemetry and
997 network analysis reveal the space use of multiple reef predators and enhance marine
998 protected area design. Proc. R. Soc. B. 283:20160717.

999 MacNeil MA, Chapman DD, Heupel M, Simpfendorfer CA, Heithaus M, Meekan M, Harvey E,
1000 Goetze J, Kiszka J, Bond ME, Currey-Randall LM, Speed CW, Sherman CS, Rees MJ, Udyawer
1001 V, Flowers KI, Clementi G, Valentin-Albanese J, Gorham T, Adam MS, Ali K, Pina-Amargós F,
1002 Angulo-Valdés JA, Asher J, Barcia LG, Beaufort O, Benjamin C, Bernard ATF, Berumen ML,

1003 Bierwagen S, Bonnema E, Bown RMK, Bradley D, Brooks E, Brown JJ, Buddo D, Burke P,
1004 Cáceres C, Cardeñosa D, Carrier JC, Caselle JE, Charloo V, Claverie T, Clua E, Cochran JEM, Cook
1005 N, Cramp J, D'Alberto B, de Graaf M, Dornhege M, Estep A, Fanovich L, Farabough NF,
1006 Fernando D, Flam AL, Floros C, Fourqurean V, Garla R, Gastrich K, George L, Graham R,
1007 Guttridge T, Hardenstine RS, Heck S, Henderson AC, Hertler H, Hueter R, Johnson M, Jupiter
1008 S, Kasana D, Kessel ST, Kiilu B, Kirata T, Kuguru B, Kyne F, Langlois T, Lédée EJI, Lindfield S,
1009 Luna-Acosta A, Maggs J, Manjaji-Matsumoto BM, Marshall A, Matich P, McCombs E, McLean
1010 D, Meggs L, Moore S, Mukherji S, Murray R, Kaimuddin M, Newman SJ, Nogués J, Obota C,
1011 O'Shea O, Osuka K, Papastamatiou YP, Perera N, Peterson B, Ponzo A, Prasetyo A, Quamar
1012 LMS, Quinlan J, Ruiz-Abierno A, Sala E, Samoilys M, Schärer-Umpierre M, Schlaff A, Simpson
1013 N, Smith ANH, Sparks L, Tanna A, Torres R, Travers MJ, van Zinnicq Bergmann M, Vigliola L,
1014 Ward J, Watts AM, Wen C, Whitman E, Wirsing AJ, Wothke A, Zarza-Gonzâlez E, Cinner JE
1015 (2020) Global status and conservation potential of reef sharks. Nature 583:801–806.

1016 Martin SM, Moir-Clark J, Pearce J, Mees CC (2013) Catch and bycatch composition of illegal
1017 fishing in the British Indian Ocean Territory (BIOT) IOTC-2013-WPEB09-46 Rev_1.
1018 http://www.iotc.org/files/proceedings/2013/wpeb/IOTC-2013-WPEB09-46%20Rev_1.pdf
1019 (accessed March 14, 2016)

1020 McCauley DJ, Young HS, Dunbar RB, Estes JA, Semmens BX, Micheli F (2012) Assessing the
1021 effects of large mobile predators on ecosystem connectivity. Ecol. Appl. 22:1711–1717.

1022 Meekan M, Cappo M, Carleton J, Marriott RR (2006) Surveys of shark and fin-fish abundance
1023 on reefs within the MOU74 Box and Rowley Shoals using baited remote underwater video
1024 systems. Australian Institute of Marine Science, Perth, Western Australia. 35 p.

1025 Mohan S, Mishra SK, Sahany S, Behera S (2021) Long-term variability of Sea Surface
1026 Temperature in the Tropical Indian Ocean in relation to climate change and variability. Global
1027 Planet. Change 199:103436.

1028 Nadon MO, Baum JK, Williams ID, McPherson JM, Zgliczynski BJ, Richards BL, Schroeder RE,
1029 Brainard RE (2012) Re-creating missing population baselines for Pacific reef sharks. Conserv.
1030 Biol. 26:493–503.

1031 Papastamatiou YP, Watanabe YY, Demšar U, Leos-Barajas V, Bradley D, Langrock R, Weng K,
1032 Lowe CG, Friedlander AM, Caselle JE (2018) Activity seascapes highlight central place foraging
1033 strategies in marine predators that never stop swimming. Mov. Ecol. 6:9.

1034 Pauly D, Cheung WWL (2017) Sound physiological knowledge and principles in modeling
1035 shrinking of fishes under climate change. Global Change Biol. 25:1.

1036 Pinheiro J, Bates D, DebRoy S, Sarkar D, R Core Team (2018) Nlme: Linear and Nonlinear Mixed
1037 Effects Models. R package version 3.1-137. https://CRAN.R-project.org/package=nlme

1038 Pohlot BG, Ehrhardt N (2017) An analysis of sailfish daily activity in the Eastern Pacific Ocean
1039 using satellite tagging and recreational fisheries data. ICES J. Mar. Sci. 75:871–879.

1040 Prince ED, Goodyear CP (2006) Hypoxia-based habitat compression of tropical pelagic fishes.
1041 Fish. Oceanogr. 15:451–464.

1042 Prince ED, Luo J, Phillip Goodyear C, Hoolihan JP, Snodgrass D, Orbesen ES, Serafy JE, Ortiz M,
1043 Schirripa MJ (2010) Ocean scale hypoxia-based habitat compression of Atlantic istiophorid
1044 billfishes. Fish. Oceanogr. 19:448–462.

1045 Queiroz N, Humphries NE, Couto A, Vedor M, da Costa I, Sequeira AMM, Mucientes G, Santos
1046 AM, Abascal FJ, Abercrombie DL, Abrantes K, Acuña-Marrero D, Afonso AS, Afonso P, Anders
1047 D, Araujo G, Arauz R, Bach P, Barnett A, Bernal D, Berumen ML, Lion SB, Bezerra NPA, Blaison
1048 AV, Block BA, Bond ME, Bradford RW, Braun CD, Brooks EJ, Brooks A, Brown J, Bruce BD, Byrne
1049 ME, Campana SE, Carlisle AB, Chapman DD, Chapple TK, Chisholm J, Clarke CR, Clua EG,
1050 Cochran JEM, Crochelet EC, Dagorn L, Daly R, Cortés DD, Doyle TK, Drew M, Duffy CAJ, Erikson
1051 T, Espinoza E, Ferreira LC, Ferretti F, Filmalter JD, Fischer GC, Fitzpatrick R, Fontes J, Forget F,
1052 Fowler M, Francis MP, Gallagher AJ, Gennari E, Goldsworthy SD, Gollock MJ, Green JR,
1053 Gustafson JA, Guttridge TL, Guzman HM, Hammerschlag N, Harman L, Hazin FHV, Heard M,
1054 Hearn AR, Holdsworth JC, Holmes BJ, Howey LA, Hoyos M, Hueter RE, Hussey NE, Huveneers
1055 C, Irion DT, Jacoby DMP, Jewell OJD, Johnson R, Jordan LKB, Jorgensen SJ, Joyce W, Daly CAK,
1056 Ketchum JT, Klimley AP, Kock AA, Koen P, Ladino F, Lana FO, Lea JSE, Llewellyn F, Lyon WS,
1057 MacDonnell A, Macena BCL, Marshall H, McAllister JD, McAuley R, Meÿer MA, Morris JJ,
1058 Nelson ER, Papastamatiou YP, Patterson TA, Peñaherrera-Palma C, Pepperell JG, Pierce SJ,

1059 Poisson F, Quintero LM, Richardson AJ, Rogers PJ, Rohner CA, Rowat DRL, Samoilys M,
1060 Semmens JM, Sheaves M, Shillinger G, Shivji MS, Singh S, Skomal GB, Smale MJ, Snyders LB,
1061 Soler G, Soria M, Stehfest KM, Stevens JD, Thorrold SR, Tolotti MT, Towner A, Travassos P,
1062 Tyminski JP, Vandeperre F, Vaudo JJ, Watanabe YY, Weber SB, Wetherbee BM, White TD,
1063 Williams S, Zárate PM, Harcourt R, Hays GC, Meekan MG, Thums M, Irigoien X, Eguíluz VM,
1064 Duarte CM, Sousa LL, Simpson SJ, Southall EJ, Sims DW (2019) Global spatial risk assessment
1065 of sharks under the footprint of fisheries. Nature 572:461–466.

1066 Queiroz N, Humphries NE, Noble LR, Santos AM, Sims DW (2010) Short-term movements and
1067 diving behaviour of satellite-tracked blue sharks *Prionace glauca* in the northeastern Atlantic
1068 Ocean. Mar. Ecol. Prog. Ser. 406:265–279.

1069 Queiroz N, Vila-Pouca C, Couto A, Southall EJ, Mucientes G, Humphries NE, Sims DW (2017)
1070 Convergent foraging tactics of marine predators with different feeding strategies across
1071 heterogeneous ocean environments. Front. Mar. Sci. 4:239.

1072 Robinson LM, Hobday AJ, Possingham HP, Richardson AJ (2015) Trailing edges projected to
1073 move faster than leading edges for large pelagic fish habitats under climate change. Deep Sea
1074 Res. Part II 113:225–234.

1075 Roman J, McCarthy JJ (2010) The whale pump: Marine mammals enhance primary
1076 productivity in a coastal basin. PLOS ONE 5:e13255.

1077 Rosa R, Rummer JL, Munday PL (2017) Biological responses of sharks to ocean acidification.
1078 Biol. Lett. 13:20160796.

1079 Roxy MK, Gnanaseelan C, Parekh A, Chowdary JS, Singh S, Modi A, Kakatkar R, Mohapatra S,
1080 Dhara C, Shenoi SC, Rajeevan M (2020) Indian Ocean Warming. In: *Assessment of Climate*
1081 *Change over the Indian Region: A Report of the Ministry of Earth Sciences (MoES), Government*
1082 *of India*. Krishnan R, Sanjay J, Gnanaseelan C, Mujumdar M, Kulkarni A, Chakraborty S (Eds)
1083 Springer, Singapore, p 191–206

1084 Royer M, Meyer C, Royer J, Maloney K, Cardona E, Blandino C, Fernandes da Silva G,
1085 Whittingham K, Holland KN (2023) “Breath holding” as a thermoregulation strategy in the
1086 deep-diving scalloped hammerhead shark. Science 380:651–655.

1087 Ryan LA, Meeuwig JJ, Hemmi JM, Collin SP, Hart NS (2015) It is not just size that matters: shark
1088 cruising speeds are species-specific. Mar. Biol. 162:1307–1318.

1089 Schielzeth H, Nakagawa S (2013) Nested by design: model fitting and interpretation in a mixed
1090 model era. Methods Ecol. Evol. 4:14–24.

1091 Sewell RBS, Fage L (1948) Minimum Oxygen Layer in the Ocean. Nature 162:949–951.

1092 Sguotti C, Lynam CP, García-Carreras B, Ellis JR, Engelhard GH (2016) Distribution of skates
1093 and sharks in the North Sea: 112 years of change. Global Change Biol. 22:2729–2743.

1094 Sims DW, Wearmouth VJ, Southall EJ, Hill JM, Moore P, Rawlinson K, Hutchinson N, Budd GC,
1095 Righton D, Metcalfe JD, Nash JP, Morritt D (2006) Hunt warm, rest cool: bioenergetic strategy
1096 underlying diel vertical migration of a benthic shark. J. Anim. Ecol. 75:176–190.

1097 Stramma L, Prince ED, Schmidtko S, Luo J, Hoolihan JP, Visbeck M, Wallace DWR, Brandt P,
1098 Körtzinger A (2012) Expansion of oxygen minimum zones may reduce available habitat for
1099 tropical pelagic fishes. Nat. Clim. Change 2:33–37.

1100 Sunday JM, Bates AE, Dulvy NK (2011) Global analysis of thermal tolerance and latitude in
1101 ectotherms. Proc. R. Soc. B 278:1823–1830.

1102 Teo SLH, Boustany A, Blackwell S, Walli A, Weng KC, Block BA (2004) Validation of geolocation
1103 estimates based on light level and sea surface temperature from electronic tags. Mar. Ecol.
1104 Prog. Ser. 283:81–98.

1105 Tickler DM, Carlisle AB, Chapple TK, Curnick DJ, Dale JJ, Schallert RJ, Block BA (2019) Potential
1106 detection of illegal fishing by passive acoustic telemetry. Anim. Biotelemetry 7:1.

1107 Tickler DM, Letessier TB, Koldewey HJ, Meeuwig JJ (2017) Drivers of abundance and spatial
1108 distribution of reef-associated sharks in an isolated atoll reef system. PLOS ONE 12:e0177374.

1109 Tolotti M, Bauer R, Forget F, Bach P, Dagorn L, Travassos P (2017) Fine-scale vertical
1110 movements of oceanic whitetip sharks (*Carcharhinus longimanus*). Fish. Bull. 115:380–395.

1111 Vedor M, Mucientes G, Hernández-Chan S, Rosa R, Humphries N, Sims DW, Queiroz N (2021)
1112 Oceanic Diel Vertical Movement Patterns of Blue Sharks Vary With Water Temperature and
1113 Productivity to Change Vulnerability to Fishing. Front. Mar. Sci. 8:688076.

1114 Vedor M, Queiroz N, Mucientes G, Couto A, Costa I da, Santos A dos, Vandeperre F, Fontes J,
1115 Afonso P, Rosa R, Humphries NE, Sims DW (2021) Climate-driven deoxygenation elevates
1116 fishing vulnerability for the ocean's widest ranging shark. eLife 10:e62508.

1117 Vetter R, Kohin S, Preti A, McClatchie S, Dewar H (2008) Predatory interactions and niche
1118 overlap between mako shark, *Isurus oxyrinchus*, and jumbo squid, *Dosidicus gigas*, in the
1119 California current. CalCOFI Rep. 49:142–156.

1120 Vianna GMS, Meekan MG, Meeuwig JJ, Speed CW (2013) Environmental influences on
1121 patterns of vertical movement and site fidelity of grey reef sharks (*Carcharhinus*
1122 *amblyrhynchos*) at aggregation sites. PLOS ONE 8:e60331.

1123 Vianna GMS, Meekan MG, Ruppert JLW, Bornovski TH, Meeuwig JJ (2016) Indicators of fishing
1124 mortality on reef-shark populations in the world's first shark sanctuary: the need for
1125 surveillance and enforcement. Coral Reefs 35:973–977.

1126 White TD, Carlisle AB, Kroodsma DA, Block BA, Casagrandi R, De Leo GA, Gatto M, Micheli F,
1127 McCauley DJ (2017) Assessing the effectiveness of a large marine protected area for reef shark
1128 conservation. Biol. Conserv. 207:64–71.

1129 Whoriskey F, Hindell M (2016) Developments in Tagging Technology and Their Contributions
1130 to the Protection of Marine Species at Risk. Ocean Dev. Int. Law 47:221–232.

1131 Williams JJ, Papastamatiou YP, Caselle JE, Bradley D, Jacoby DMP (2018) Mobile marine
1132 predators: an understudied source of nutrients to coral reefs in an unfished atoll. Proc. R. Soc.
1133 B 285:20172456.

1134 Worm B, Tittensor DP (2011) Range contraction in large pelagic predators. PNAS 108:11942–
1135 11947.

1136 Zuur AF, Ieno EN, Walker NJ, Saveliev AA, Smith GM (2009) Mixed Effects Modelling for
1137 Nested Data. In: *Mixed effects models and extensions in ecology with R*. Statistics for Biology

and Health, Zuur AF, Ieno EN, Walker N, Saveliev AA, Smith GM (eds) Springer, New York, NY, p 101–142

Tables

Table 1: Summary of pop-up satellite archival tag (PAT) deployments on silvertip sharks in the BIOT MPA in 2013 and 2014.

	Shark metadata					Deployment			Pop-off			Tag programming				Tag reporting			
Tag	Tag ID	Sex	PCL (cm)	FL (cm)	TL (cm)	Date	Lat (°N)	Lon (°S)	Date	Lat (°N)	Lon (°S)	Days planned	Days active	% active	Histo-gram interval (hrs)	Max depth (m)[1]	Days data	TS data	MLD
1	391300800[2]	-	141	155	185	12/02/13	-5.34	71.98	11/08/13	-5.32	72.00	180	180	100	24	594±6	179	Y	Y
2	391301000	-	122	134	160	16/03/13	-5.26	72.44	27/07/13	-5.91	71.35	270	133	49	24	488±4	87		Y
3	391301400	-	122	134	160	12/03/13	-5.27	72.44	06/07/13	-5.26	71.67	180	116	64	6	760±4	104		Y
4	391303300	-	113	124	148	22/03/13	-5.27	71.67	04/07/13	-5.24	71.66	180	105	58	24	792±4	105		Y
5	391400800[3]	F	129	139	161	24/03/14	-5.37	72.22	22/07/14	-5.04	73.02	120	120	100	24	464±4	102	Y	
6	391401600[4]	F	110	124	145	25/03/14	-5.30	72.25	30/07/14	-5.29	71.72	180	127	71	6	400±4	107		Y
7	391401800[3]	F	109	120	150	27/03/14	-5.55	72.22	06/07/14	-4.87	74.12	180	101	56	24	328±4	86	Y	

Notes:

[1] Max depth estimates obtained from daily temperature and depth summaries or directly from tag series data.

[2] Tag 391300800 was physically recovered, allowing the full on-board data archive to be downloaded (15 second-interval time series).

[3] Tags 391400800 and 391401800 transmitted time series data, sampled from the on-board data archive at 5 and 7.5 minute intervals, respectively.

[4] Tag 391401600 was tagged with both a PAT and a Vemco V16 acoustic tag.

Acronyms used in table header: PCL – Precaudal length, FL- fork length, TL – total length, Lat – Latitude, Lon - Longitude

Table 2: Proportion of time spent by tagged silvertip sharks below given depth and temperature thresholds. Mean proportion of time (± 95% CI) spent below a threshold reported overall, and separately for day and night time periods. T-test results for difference between day and night proportions are shown in last columns.

Threshold	Proportion of time period spent below threshold depth or temperature (± 95% CI)			t	df	p-value
	Overall %	Daytime %[1]	Night time %[2]			
Depth						
75m	5.1 ± 0.5	9.1 ± 0.9	4.1 ± 0.6	-6.64	567.77	< 0.001
100m	1.5 ± 0.1	1.8 ± 0.3	1.1 ± 0.1	-3.56	559.63	< 0.001
150m	0.3 ± 0.1	0.3 ± 0.1	0.4 ± 0.1	3.01	757.64	0.002
Temperature						
25°C	20.4 ± 0.8	33.0 ± 1.7	14.5 ± 0.9	18.89	838.02	0.001
22°C	6.4 ± 0.5	11.3 ± 1.0	4.1 ± 0.4	13.35	745.46	0.001
18°C	1.1 ± 0.1	1.2 ± 0.2	0.9 ± 0.1	2.52	635.78	0.012

1. Daytime: 06:00-18:00; 2. Night time: 18:00 – 06:00

Table 3: Fixed effects of highest ranked GLMMs modelling the semi-diel (day/night) depth of silvertip sharks in BIOT. Candidate fixed effects were mixed layer depth (MLD: metres), sea surface temperature (SST: °C), time of day (TOD), lunar phase (Moon: new, waxing, full, waning) and shark total length (TL: cm). The predictors' estimated coefficients (and standardised beta values) for each of the six candidate models are shown, below the models' AICc score and marginal R^2. Predictors and/or interactions with t test p-values less than 0.05 indicated in bold.

Model: Depth ~	**MLD + TOD + TL**	**MLD + TOD**	**MLD + TOD + SST**	**MLD + TOD*Moon + TL**	**MLD + TOD*Moon + SST**	**MLD + TOD*Moon + SST + TL**
AICc	6335.2	6335.5	6336.4	6337.9	6339	6339.1
R^2m[a]	0.32	0.27	0.28	0.34	0.29	0.34
Fixed effects[b]						
(Intercept)	2.39	**26.47**	3.15	4.22	3.96	-16.16
MLD	**0.33 (0.29)**	**0.33 (0.29)**	**0.33 (0.30)**	**0.33 (0.29)**	**0.33 (0.29)**	**0.33 (0.29)**
SST	-	-	0.81 (0.04)	-	0.85 (0.04)	0.73 (0.03)
Night	**-9.97**	**-9.98**	**-9.99**	**-12.54**	**-12.57**	**-12.55**
MoonWaxing	-	-	-	-2.01	-1.95	-1.97
MoonFull	-	-	-	**-3.36**	**-3.31**	**-3.33**
MoonWaning	-	-	-	-2.51	-2.55	-2.56
TL	0.15 (0.16)	-	-	0.15 (0.16)	-	0.15 (0.16)
Night:MoonWaxing	-	-	-	2.09	2.11	2.10
Night:MoonFull	-	-	-	**5.48**	**5.50**	**5.49**
Night:MoonWaning	-	-	-	2.40	2.40	2.40

a. Marginal R^2 (R^2m, Schielzeth and Nakagawa 2013) is an estimate of the variance explained by the fixed effects in a mixed-effects model.
b. Standardised (beta) parameter estimates are shown in brackets for continuous predictors.

Figures

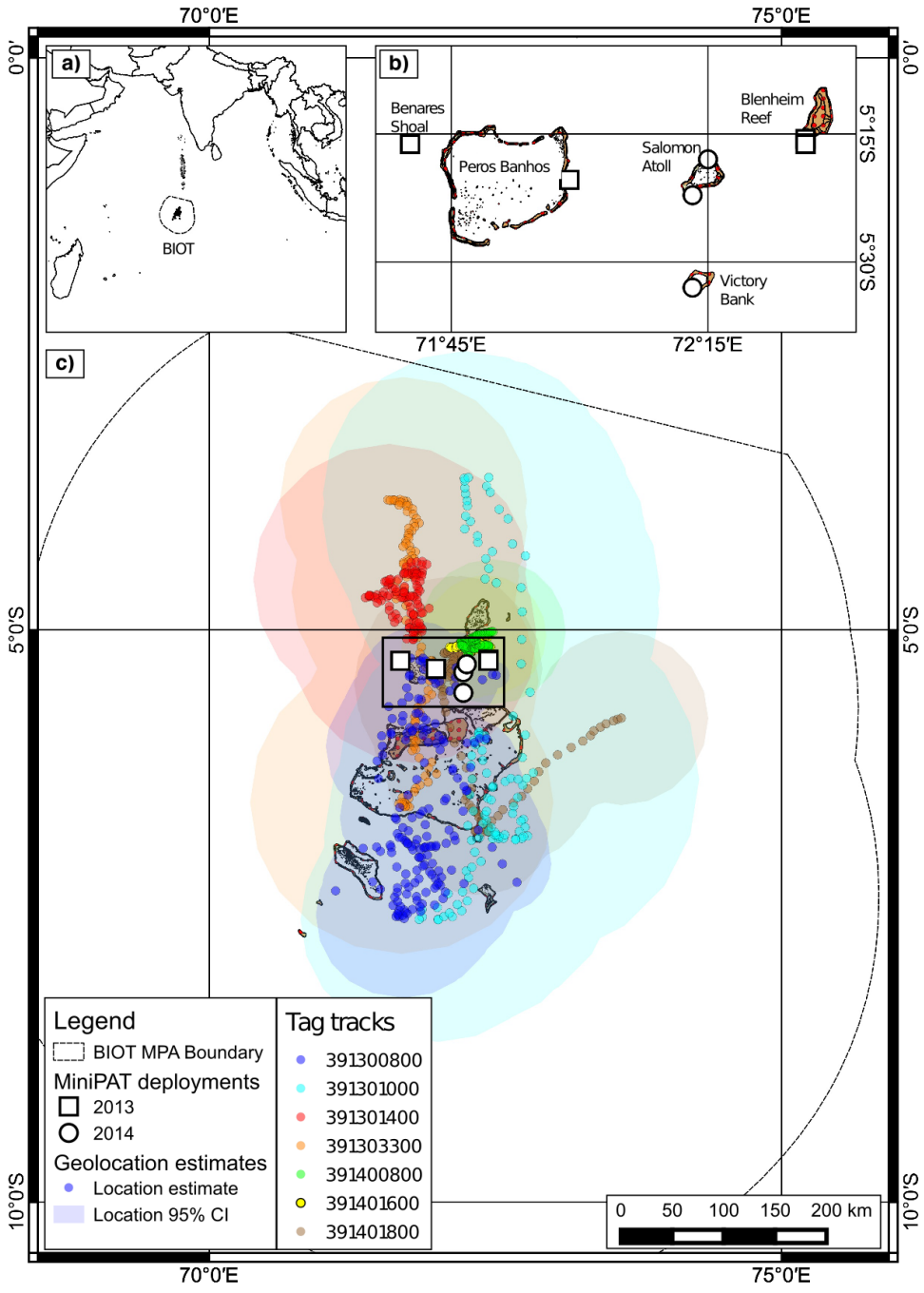

Figure 1: Map of study area showing a) location of the BIOT EEZ in the Indian Ocean; b) locations of seven PAT tag deployments on silvertip sharks in 2013 (squares, n=4) and 2014 (circles, n=3); and c) daily geolocation-based position estimates and their 95% confidence areas, for all seven tags colour coded by tag ID as per legend.

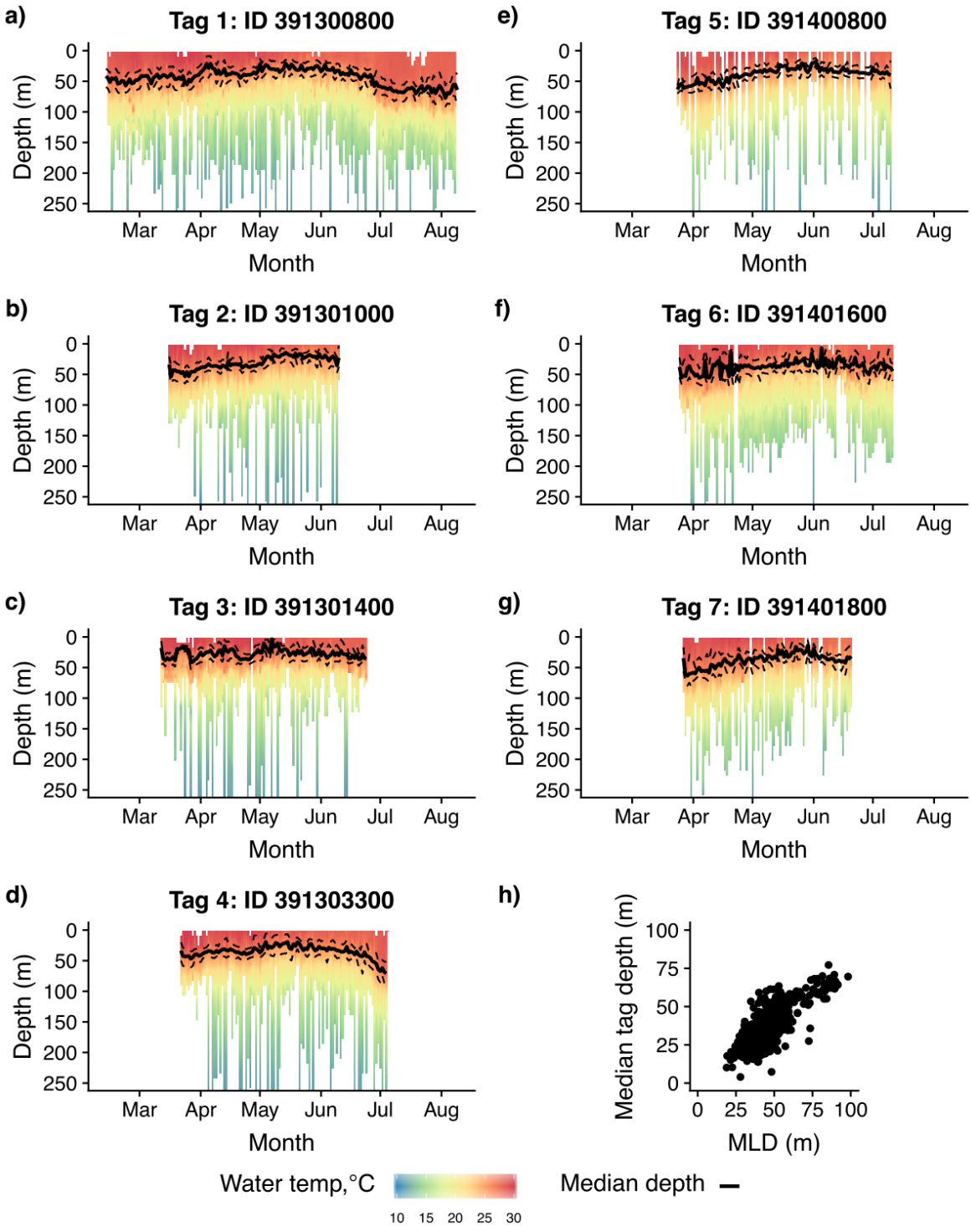

Figure 2: Bathythermographs (a-g) based on daily depth and temperature records for seven silvertip sharks tagged in 2013 (a-d) and 2014 (e-g). Depth range has been truncated to show greater detail. Solid line indicates median daily depth for each shark; dashed lines show upper and lower quartiles of daily depth distribution. Colour indicates ambient water temperature recorded by tags. Panel h) shows overall relationship between median daily depth and mixed layer depth (MLD), pooled for all sharks (Pearson's correlation = 0.77).

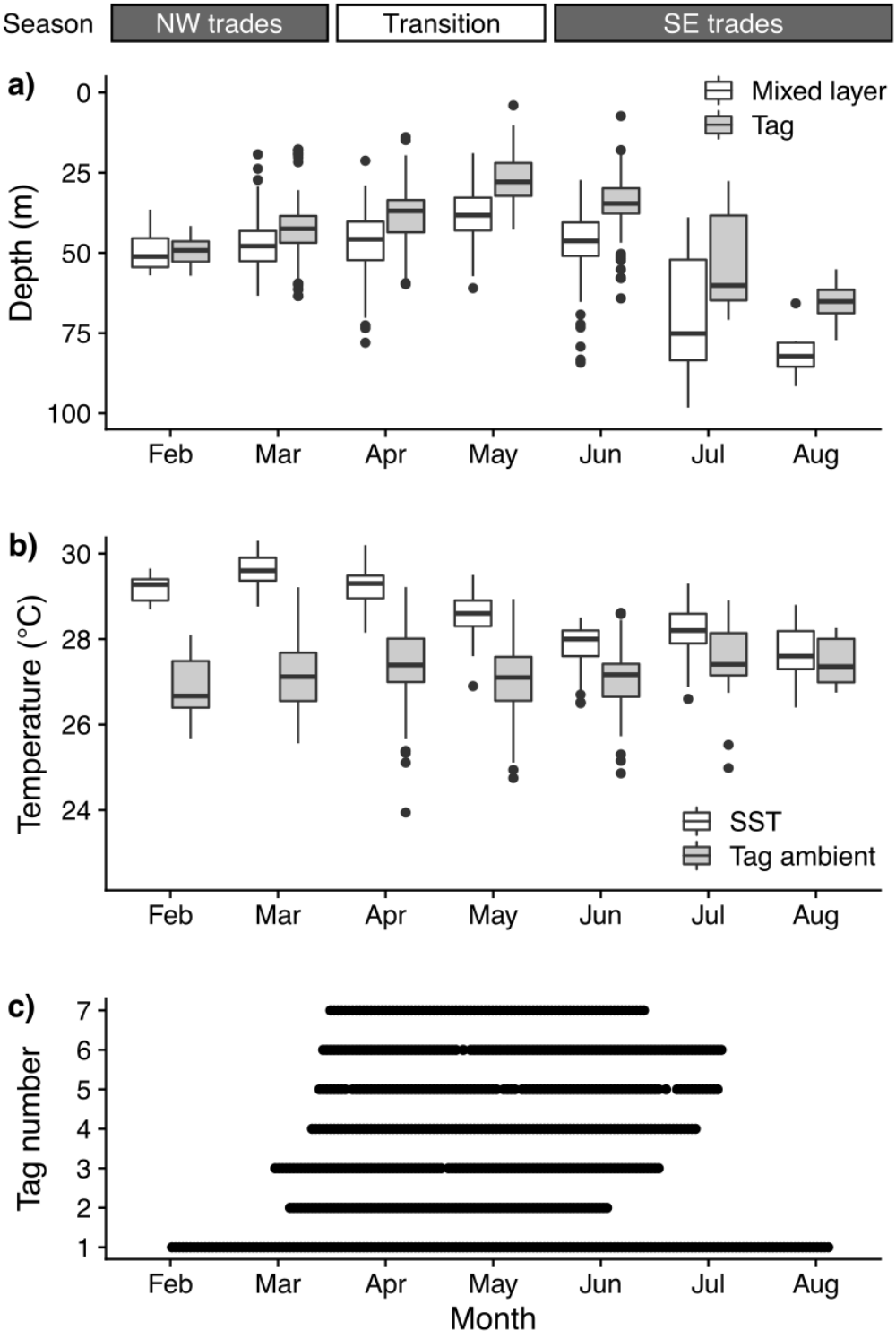

Figure 3: Boxplots by month of a) daily mix layer depth and daily median tag depth (grey fill) and b) daily mean sea surface temperature (SST) and daily median tag ambient temperature (grey fill), pooled across tags (n = 7) and years. Heavy horizontal line is monthly median; box indicates IQR; whiskers = 95% range; outliers plotted individually. Panel c) shows distribution of data records over time for each tag, with time series aligned by calendar month.

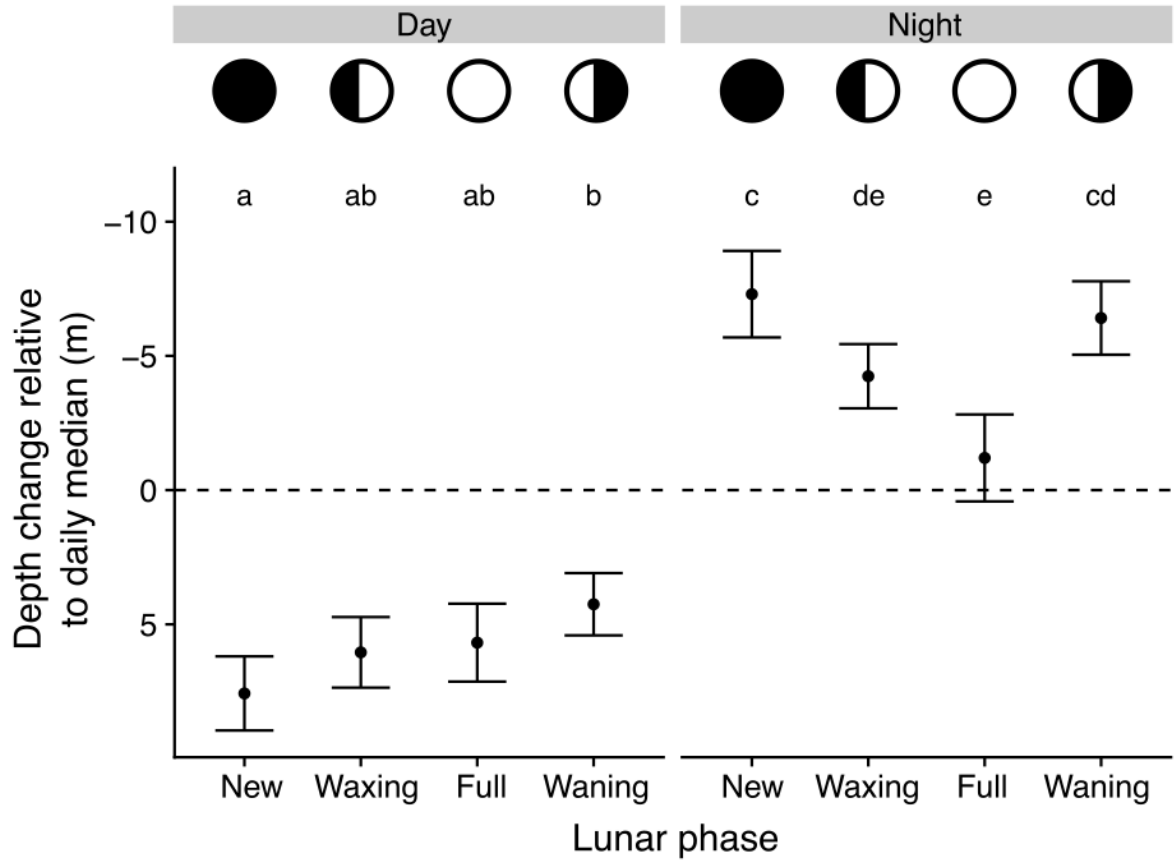

Figure 4: Change in the median depth occupied by five silvertip sharks with time of day (day or night) and lunar phase, adjusted for seasonal variation. Error bars indicate 95% confidence interval of mean values for all sharks. Changes in median depths are standardised relative to each shark's 30-day rolling median depth. Lowercase letters above plot indicate results of Tukey's test for Honestly Significant Difference for an analysis of variance test of depth change against time of day, lunar phase and their interaction. Factor combinations labelled with the same letter are not significantly different at the 5% level.

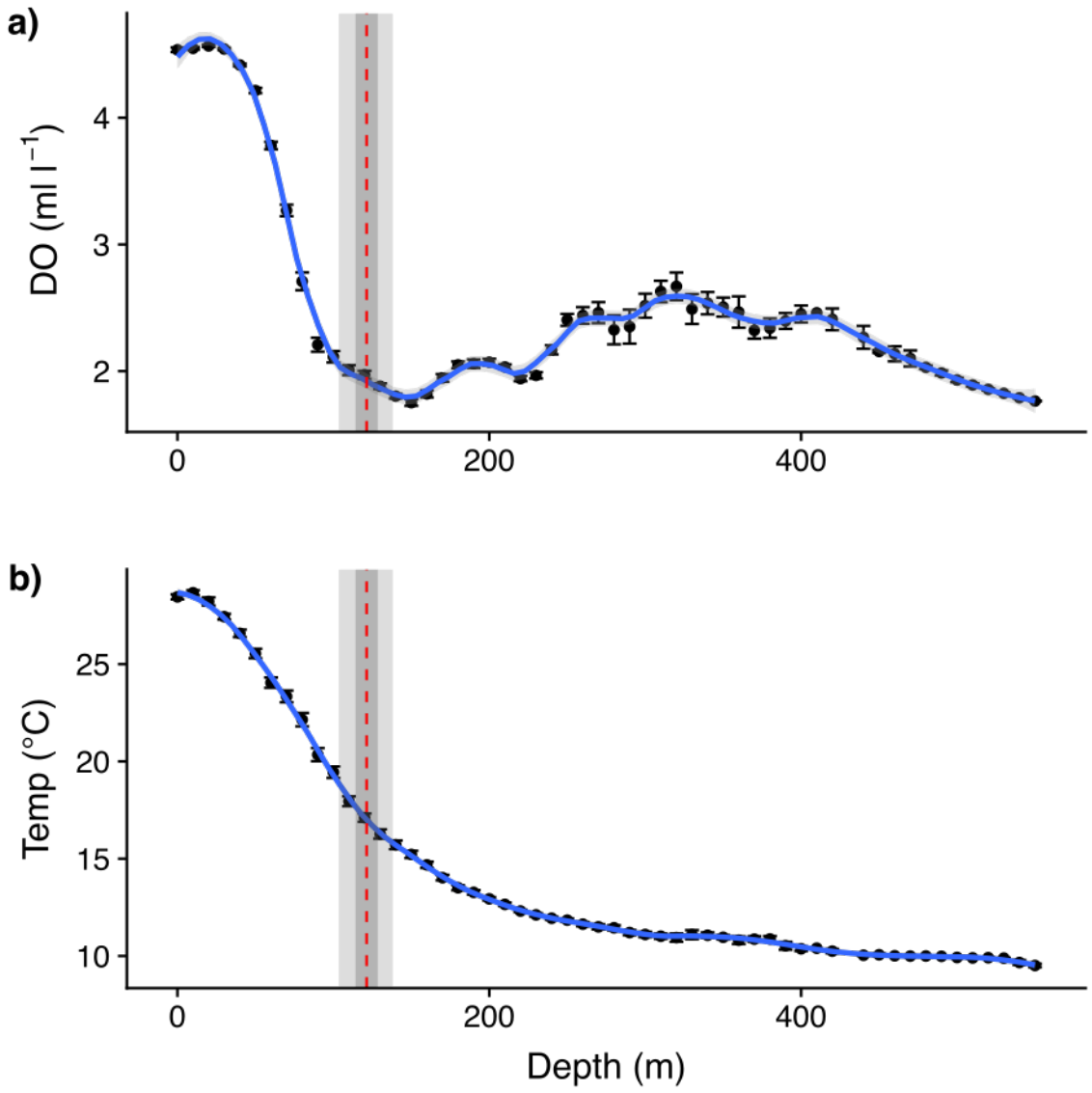

Figure 5: Average dissolved oxygen (a) and temperature (b) profiles for the deep dives (i.e. where max depth was > 200 m) recorded for a single silvertip shark (Tag 1, ID 391300800). Dashed vertical red line indicates the mean depth of the ascent rate transition point in ascents from these dives. Dark and light shaded bands indicate CI and IQR of transition point depth, respectively.